



Decadal trends in seasonal streamflow and stream temperature across the United States

Timothy J. Stagnitta¹, Zachary C. Johnson², Brian A. Ebel³, Jessica R. Ayers⁴

¹U.S. Geological Survey – New York Water Science Center, Cortland, NY, 13045, USA

5 ²U.S. Geological Survey – Washington Water Science Center, Tacoma, WA, 98402, USA

³U.S. Geological Survey – Water Resources Mission Area, Burlington, VT, 05405, USA

⁴The Nature Conservancy, San Francisco, CA, 94111, USA

Correspondence to: Timothy J. Stagnitta (tstagnitta@usgs.gov)



Abstract.

Streamflow influences water supply and hydrologic extremes, whereas stream temperature controls thermal conditions critical for aquatic species. Changes in streamflow and stream temperature have far reaching ecological and socioeconomical implications; thus, it is essential to understand their interconnected seasonal trends and relation to external forcing factors. In this analysis, we (1) documented and compared decadal trends (1980-2020, 1990-2020, and 2000-2020) in seasonal and annual streamflow and stream temperature metrics at sites across the conterminous United States (CONUS), Alaska, Hawaii, and Puerto Rico; (2) assessed land cover, precipitation, air temperature, and baseflow fraction effects on streamflow and stream temperature; and (3) selected three hydrologic regions (Midwest, California-Nevada, and Atlantic Coast) within CONUS as regional case studies to better understand the effects of climate and land-use drivers on streamflow and stream temperature. Trends were evaluated using the following likelihood categories: likely ($p_t \leq 0.1$), somewhat likely ($0.33 \geq p_t > 0.1$), uncertain ($0.67 \geq p_t > 0.33$), and unlikely ($0.67 > p_t$), where p_t is the p-value determined from the Mann-Kendall trend test. Most trends were uncertain or unlikely, but some significant changes were found, such as positive correlations between air temperature and rising stream temperatures and between precipitation and increasing streamflow. Streamflow increased across most of CONUS for the 2000-2020 period, but decreases were more prominent for the 1980-2020 and 1990-2020 trend periods across the southern and western CONUS. During the 2000-2020 trend period, seasonal trends in increasing stream temperature were attributed to warmer summer and fall air temperature. Increasing seasonal streamflow was attributed to increases in precipitation in the winter and spring and decreases in baseflow fraction during the spring and summer seasons. We show streamflow trends vary in direction across different trend periods for multiple U.S. regions, which poses challenges for water resources planning and management. Regional results indicated that increasing streamflow in the Midwest region was attributed to increasing precipitation and decreasing baseflow fraction across all seasons. Decreasing streamflows in the California-Nevada region were associated with increasing spring baseflow fraction and increasing annual air temperature. Increasing and decreasing stream temperatures in the Atlantic Coast region were attributed to both increasing and decreasing air temperature, respectively. This study emphasizes the importance of studying streamflow and stream temperature together and demonstrates how comparisons of seasonal and annual metrics provide a more nuanced analysis of streams than annual metrics alone.

1 Introduction

Understanding how and why streamflow and stream temperature are changing are pressing issues with far reaching ecological and socioeconomic implications because they play a critical role in water quality and freshwater ecosystems. Streamflow and stream temperature separately and jointly govern key physical and chemical processes (e.g., nutrient transport, sediment deposition and habitat availability) and physiological suitability for aquatic species (e.g., availability of dissolved oxygen and other gases, Johnson et al., 2024; Zhi et al., 2023). Furthermore, these variables are often seasonally synchronized where peak flows often coincide with cooler temperatures (Dudley et al., 2017; Ford et al., 2021; Uzun et al., 2021) and low



flows with maximum stream temperatures (Constantz, 1998; Arismendi et al., 2013). As a result, climate and land use change could potentially have compounding impacts (IPCC, 2023; Kaushal et al., 2010). Although recent studies have documented significant changes in streamflow (Ficklin et al., 2016; Ayers et al., 2022; Singh and Basu, 2022) and stream temperature (Kelleher et al., 2021) independently across conterminous United States (CONUS), changes in streamflow and stream temperature have not been broadly studied together. Thus, it remains unclear how changes in streamflow either mirror or diverge from changes in stream temperature across the United States.

Across CONUS, observed warming air temperature (e.g., Vose et al., 2017; IPCC, 2023) and changes in streamflow timing and magnitude (e.g., Ficklin et al., 2016; Gupta et al., 2023; Ayers et al., 2022; Hidalgo et al., 2009; Dudley et al., 2017) have been hypothesized to cause increases in the magnitude and variability of stream temperature in recent decades (e.g., Isaak et al., 2012; Rice and Jastram, 2015; Tassone et al., 2023). However, to our knowledge, few studies have examined broad scale changes in stream temperature (e.g., Kaushal et al., 2010; Kelleher et al., 2021) and focused only on air temperature and land use characteristics as causal mechanisms rather than streamflow (e.g., Kaushal et al., 2010). Additionally, most studies analysing the relationship between streamflow and stream temperature have done so at individual watersheds in the context of understanding their impact on fish populations (e.g., Isaak et al., 2012; Morales-Marin et al., 2019; Santiago et al., 2017). While these studies highlight the importance of both factors on aquatic ecosystem dynamics (e.g., dissolved oxygen and stream greenhouse gas production), their small scale limits their ability to find patterns across broader spatial scales.

Numerous studies have examined CONUS scale changes in streamflow (e.g., Ficklin et al., 2016; Barnett et al., 2008; Dudley et al., 2017; Stewart et al., 2005; Ford et al., 2021; Ayers et al., 2022; Ayers et al., 2021; Zipper et al., 2021; Dudley et al., 2020; Wang et al., 2024). These studies pointed to changes in streamflow timing and magnitude likely related to earlier peak flow in the spring from warmer air temperature (e.g., Ayers et al., 2022; Zipper et al., 2021; Stewart et al., 2005; Ford et al., 2021) and land use change (e.g., Ayers et al., 2021; Dudley et al., 2020; Singh and Basu, 2022; Rice et al., 2015). While these studies underscore the potential impact of changes in streamflow seasonality, they have not been linked to seasonal stream temperature dynamics. Furthermore, studies often highlight the importance of confounding influencing factors yet lack a comprehensive analysis of a large suite of factors, especially land use changes (e.g., Kaushal et al., 2010; Lins and Slack, 2005; Singh and Basu, 2022; van Vliet et al., 2011; Ayers et al., 2021). Understanding the relationship between seasonal trends in streamflow and stream temperature and their relationship with forcing factors is essential to understand ecosystem health under environmental changes.

To address the abovementioned challenges, this study explores seasonal trends in stream temperature and streamflow across CONUS, Alaska, Hawaii, and Puerto Rico (United States). Our objectives were to first characterize decadal trends in seasonal and annual streamflow and stream temperature for three trend periods (1980-2020, 1990-2020, and 2000-2020). Next, we use correlation to evaluate the impact of land cover, precipitation, air temperature, and baseflow fraction on streamflow and stream temperature. Finally, we select three hydrologic regions (California-Nevada, Midwest, and Atlantic Coast) within CONUS to demonstrate the effects of climate and land-use drivers on streamflow and stream temperature at the regional scale.



2 Methods

Stream temperature trends data for this study were available from a U.S. Geological Survey (USGS) data release for stream temperature metrics and trends (Johnson, 2025). Stream temperature trend results were calculated from mean, minimum, and maximum daily stream temperature available from 2,213 monitoring stations collated by Oliver et al. (2024) from the U.S. Environmental Protection Agency Water Quality Portal (Read et al., 2017), USGS National Water Information System (NWIS; USGS, 2021), Spatial Hydro-Ecological Decision System (<http://db.ecosheds.org/>), and the U.S. Department of Agriculture NorWeST database (Isaak et al., 2017). Streamflow trends data for this study were available from a USGS data release related to streamflow trends (Hecht et al., 2024). Streamflow trend results were calculated from mean daily discharge for 6,347 USGS streamgages from USGS NWIS. Hecht et al. (2024) and Johnson (2025) both include trends calculated over three periods: 1980-2020, 1990-2020, and 2000-2020 available across the United States. In total, the initial dataset includes 7,663 sites within CONUS and 170 sites outside of CONUS. The metrics we used for stream temperature (degrees Celsius; °C) included the annual mean, annual maximum of the moving 7-day average maximum temperature (high7dmax), annual minimum of the moving 7-day average minimum temperature (low7dmin), and the monthly mean (Johnson, 2024; Oliver et al., 2024). The metrics used for streamflow (cubic feet per second; ft³/s) included the annual mean, annual maximum moving 7-day average (high7d), annual minimum moving 7-day average (low7d), and the monthly mean (Hecht et al., 2024). The annual low7dmin and low7d metrics were calculated using the climate year (April-March), and the annual high7dmax, high7d, and annual mean were calculated using the water year (October-September). A climate year is assigned to the calendar year in which the 12-month period from April 1 to March 31 ends, and a water year is assigned to the calendar year in which the 12-month period from October 1 to September 30 ends. To check for record completeness, Johnson (2024) and Hecht et al. (2024) analysed time series for trend analyses based on two requirements: (1) values for at least 80% of the trend period (i.e., eight of every 10 years) and (2) values in at least 8 out of the first and last 10 years of the trend period, respectively. Additionally, USGS locations with known upstream reservoirs include only post-reservoir construction periods determined by Headman and Hecht (2024) to avoid abrupt changes within the period of record (non-USGS locations were not evaluated for reservoir impacts). Sites from sources other than USGS NWIS may not have upstream reservoirs identified. Additional information on methods used to prepare the stream temperature and streamflow trend datasets are provided in Johnson (2024) and Hecht et al. (2024), respectively. Also, the trends data available from these data releases were organized for use in this study by Stagnitta et al. (2026).

Modified CONUS level-4 hydrologic unit code (HUC) based regions were used to define sites within each region, including Alaska, Hawaii, and Puerto Rico as separate regions following Van Metre et al. (2020). A total of 18 hydrologic regions were defined in CONUS, and the state boundaries of states outside CONUS were used as separate boundaries (Fig. A14). The hydrologic regions were developed to support intensive monitoring and assessment of priority river basins by the USGS. We selected three hydrologic regions (Midwest – hydrologic region 5, California-Nevada – hydrologic region 18, and Atlantic Coast – hydrologic region 2) to discuss regional trends of streamflow and stream temperature. These regions were



selected based on consistent increasing or decreasing streamflow trends and stream temperature data availability across all
110 trend periods. The streamflow and stream temperature datasets were processed using R statistical software version 4.3.2 and
4.4.0, respectively (R Core Team, 2025).

2.1 Driver Datasets

Basins were delineated using the 'pynhd' package v0.18.0 in the HyRiver software stack (Chegini et al., 2021) in
Python 3.13. Basin geometries from the 6,859 sites (90% of the total) associated with USGS streamgages were derived from
115 the Hydro Network-Linked Data Index (NLDI; U.S. Geological Survey, 2025). The 795 sites (10% of the total) not associated
with USGS streamgages had basin geometries estimated using the nearest common identifier (COMID) from the National
Hydrography Dataset Plus (NHDPlus; USGS, 2022). COMIDs encompass a collection of data that fully describe NHDPlus
basins, including geometries (Blodgett and Johnson, 2022). There is some additional uncertainty in the estimated watersheds
delineation geometry for non-USGS streamgage locations because the nearest COMID may be separated from the actual
120 location.

Gridded climate data were obtained from the Parameter-Elevation Regressions on Independent Slopes Model
(PRISM) gridded climate dataset from 1981-2020 (PRISM Group, 2014). We used the monthly average precipitation and
temperature from the PRISM dataset provided at a 4-km spatial resolution across 7,322 basins within CONUS. The 'prism'
v0.2.3 R package (Hart and Bell, 2015) was used to download the monthly gridded datasets for CONUS. Next, the 'terra' v1.8-
125 42 R package (Hijmans, 2025) was used to extract and calculate the basin-wide average of the monthly mean precipitation and
temperature using the delineated basins. In addition, the PRISM dataset was used to develop a regional climate comparison of
potential bias in starting and ending years for each trend period, where the trend period years were compared to the 1991-2020
climate normal, and z-scores were calculated across all PRISM pixel values within each hydrologic region. The non-parametric
Wilcoxon test was used to determine the significance (p -value < 0.05) between each starting year and 2020, where starting
130 years that were significantly different from 2020 were used to help describe the sensitivity of the starting year within each
trend period.

Annual land cover data were obtained from the National Land Cover Database (NLCD; USGS, 2024). The NLCD
dataset contains annual land cover information across CONUS from 1985-2023. The dataset is produced from legacy 30-m
Landsat images, chained deep learning models, and harmonic time series analysis (USGS, 2024). Land cover information was
135 classified into the following categories: water, developed, barren, forest, shrubland, herbaceous, planted/cultivated, and
wetlands (Anderson et al., 1976). The 'terra' R package (Hijmans, 2025) was used to count the number of pixels and calculate
the percentage of each land cover class for each delimited basin by year across 7,322 sites within CONUS.

Daily baseflow data were obtained from Konrad (2022) for 13,208 streamgage sites across the United States derived
from a non-linear baseflow separation model. The methods from Johnson (2024), Hecht et al. (2024), and Headman and Hecht
140 (2025) were used to filter sites with baseflow data for complete datasets and post-reservoir construction periods. The annual
and monthly average baseflow fractions were calculated for 4,995 basins across all years of data. The driver datasets were



processed using the R statistical software version 4.4.3 (R Core Team, 2025). Refer to table 1 for an organized list of input data sources described in this section.

Table 1: The input data sources for this project.

Input data source	Citation	Metrics	Trend periods	Spatial resolution
Stream temperature	Johnson, 2024	Annual mean, low7dmin, high7dmax, and monthly mean	1980-, 1990-, and 2000-2020	Point location
Streamflow	Hecht et al, 2024	Annual mean, low7d, high7d, and monthly mean	1980-, 1990-, and 2000-2020	Point location
Modified CONUS level-4 HUC based regions	Van Metre et al., 2020	NA	NA	Level-4 HUC regions
Delineated basins	USGS, 2025 and Blodgett and Johnson, 2022	NA	NA	NA
PRISM Air Temperature and Precipitation	PRISM Group, 2014	Annual and monthly mean	1980-, 1990-, and 2000-2020	4 km grid cells
Annual NLCD	USGS, 2024	Annual percentage of land cover	1990- and 2000-2020	Derived from 30-m Landsat images
Modelled daily baseflow fraction	Konrad, 2022	Annual and monthly mean	1981-, 1990-, 2000-2020	Point location

145

2.2 Statistical analyses

Johnson (2024) and Hecht et al. (2024) used Mann-Kendall (Mann, 1945; Kendall, 1948) monotonic trend analysis (Helsel et al., 2020) to calculate streamflow and temperature trends for sites across the United States. In addition, the presence of serial correlation was determined using an autoregressive integrated moving average (ARIMA) model with a lag-one correlation of the detrended time series and a hypothesis test to determine if the time series was independent or autocorrelated. For example, if an ARIMA model with a lag-one correlation of the detrended time series produced a lower Akaike Information Criterion (AIC) with a small-sample correction and a no lag model, the null hypothesis of autocorrelated was used; otherwise,

150



the null hypothesis of independence was applied. The magnitude of trends was calculated using the Theil-Sen slope method (Theil, 1950; Sen, 1968), which is the median of all pairwise slope annual values for each metric (Helsel et al., 2020). These methods were also used to calculate trends in the driver datasets: annual NLCD, PRISM precipitation and air temperature, and baseflow fraction (Stagnitta et al., 2026; Table 1).

We report trends using trend likelihood categories because of the broad scale of site locations, and p-values are used as a measure of trend significance. The categories were defined using p-values as follows: “likely” is less than or equal to 0.1, “somewhat likely” is between 0.1 and 0.33, “uncertain” is between 0.33 and 0.67, and “unlikely” is greater than 0.67 (Hirsch et al., 2015; Mastrandrea et al., 2010). The sign of the Theil-Sen slope was used to define the direction of the trend as either increasing (positive) or decreasing (negative). Next, we determined the Kendall rank-based correlation (Hollander et al., 2015) between the monthly and annual metrics of the driver, streamflow, and stream temperature datasets. Finally, the correlation analysis and the trend of each driver dataset was used to determine the attribution evidence to describe the monthly and annual streamflow and stream temperature trends (Table 2; Ryberg, 2022). For example, at one site, if the trend test for mean April precipitation was likely increasing ($p_t \leq 0.1$), and its correlation with mean April streamflow was significant ($p_c < 0.05$), this is interpreted as robust evidence that increasing April precipitation influences increasing April streamflow.

Table 2: Trend likelihood category (Hirsch et al., 2015; Mastrandrea et al., 2010) and attribution-evidence confidence categories (Ryberg, 2022) for combinations of explanatory variable correlation significance and monotonic trend significance. The variable trend significance confidence categories are also used to categorize streamflow and stream temperature trends and trend alignment. Based upon the approach used in Ryberg (2022). The p_t = trend significance, and p_c = correlation significance.

	Explanatory trend likelihood category			
	<i>Unlikely</i>	<i>Uncertain</i>	<i>Somewhat likely</i>	<i>Likely</i>
	$0.67 > p_t$	$0.67 \geq p_t > 0.33$	$0.33 \geq p_t > 0.1$	$p_t \leq 0.1$
Correlation significance	Explanatory trend significance evidence category			
$p_c > 0.1$	Unknown	Unknown	Unknown	Unknown
$0.10 \geq p_c \geq 0.05$	Unknown	Limited	Moderate	Moderate
$p_c < 0.05$	Unknown	Limited	Moderate	Robust

3 Results

Seasonal and annual trends across the United States for stream temperature and streamflow across multiple trend periods are presented in the following sections.



175 3.1 Stream temperature trends

Stream temperature data were scarcer than streamflow data because they are typically measured irregularly (i.e., weekly, monthly, seasonally) and more often in warmer months. As a result, the number of sites with available data varied by months. Overall, the number of unique sites with any available monthly mean stream temperature trends data increased over more recent trend periods, probably due to the widespread availability of affordable sensors. There were 52 sites in the 1980-180 2020 period (11 with all months), 110 sites for 1990-2020 (32 with all months), and 364 sites for 2000-2020 (148 with all months; Fig. 1). Additionally, the annual mean metric had the lowest total percentage of sites because this required continuous monitoring over an entire year. For the three trend periods, there were 26, 68, and 244 sites with annual mean temperature trend data, respectively.

Generally, there were five to nine times more sites showing increasing (warming, $p \leq 0.33$) annual mean stream-185 temperature trends than decreasing (cooling, $p \leq 0.33$) trends across all trend periods in CONUS and Alaska (Fig. 1). Warming trends had mean slopes of +0.18 to +0.46 °C per decade, whereas cooling trends had mean slopes of -0.21 to -0.42 °C per decade. However, for the most recent trend period, the warming trends were less pronounced, and uncertain trends became more common. From the 1980-2020 to 1990-2020 to 2000-2020 trend periods, the fraction of increasing annual mean trend sites decreased (63%, 57%, 36%, respectively), the fraction of uncertain or unlikely ($p > 0.33$) trend sites increased (29%,190 37%, and 58%, respectively), and the fraction of decreasing trend sites remained relatively consistent (8%, 6%, and 7%, respectively).

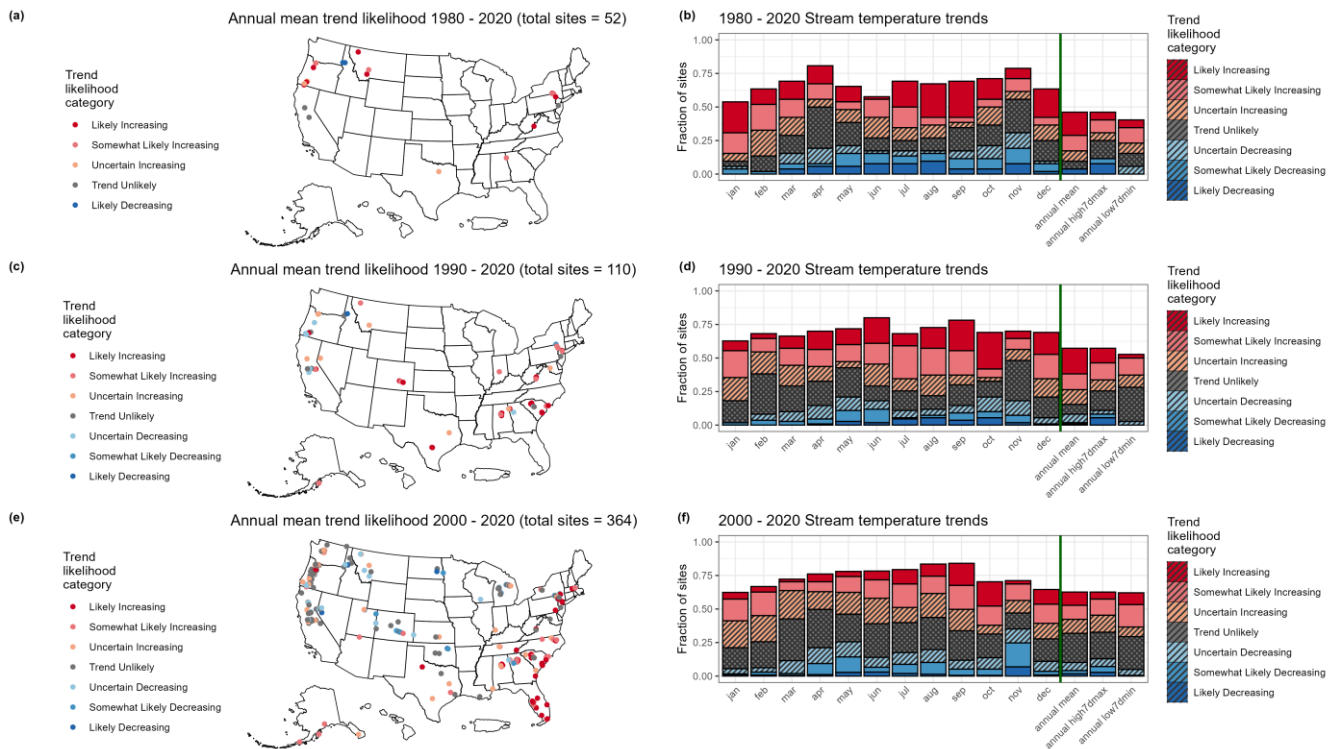
The annual high7dmax metric trend patterns were similar to those of the annual mean, while the annual low7dmin metric trend patterns showed somewhat greater uncertainty except for the most recent trend period. The annual high7dmax metric had increasing trends (likely or somewhat likely, $p \leq 0.33$) at 35%, 37%, and 25%; decreasing trends at 35%, 18%, and195 19%; and uncertain or unlikely trends at 30%, 45%, and 56% of sites for the 1980-2020 ($n=23$), 1990-2020 ($n=60$), and 2000-2020 ($n=224$) periods, respectively. The annual low7dmin metric had increasing trends at 48%, 34%, and 42%; decreasing trends at 0%, 2%, and 1%; and uncertain or unlikely trends at 52%, 64%, and 56% of sites for the 1980-2020 ($n=21$), 1990-2020 ($n=58$), and 2000-2020 ($n=226$) periods, respectively. Generally, likely trends in the annual mean and high7dmax metrics were more common during the 1980-2020 and 1990-2020 trend periods than in the low7dmin metrics across all trend periods200 and trends during the most recent trend period (2000-2020). Additionally, across all trend periods within each individual annual metric, increasing annual low7dmin is more common than decreasing trends, while the annual mean and high7dmax were about equal between increasing and decreasing trends.

Summer monthly trends were most associated with the annual mean and high7dmax trends. The late summer and early fall months of August and September consistently had the greatest fraction of sites with likely warming trends across the205 three trend periods. However, the 1980-2020 and 1990-2020 trend periods had more months throughout the year with likely warming trends than the most recent 2000-2020 trend period. The month of November for the 1980-2020 and 2000-2020 trend



periods had the largest fraction of sites with likely cooling trends. Uncertain or unlikely monthly mean stream temperature trends were the most common category across months for the 2000-2020 trend period.

210 Generally, warming annual mean trends were prominent for the eastern CONUS across all three trend periods. Also, warming annual mean trends were observed in the Pacific Northwest, which showed warming trends during 1980-2020, with more mixed results in more recent trend periods. Cooling annual mean trends were less widespread but observed in the northern Rocky Mountains and Sierra Nevada areas, and in the upper Midwest from 2000-2020. Southeastern Alaska and the Alaska Peninsula (4 sites) also showed significant warming annual mean trends from 2000-2020.



215

220 **Figure 1: Stream temperature trends by fixed trend periods of 1980-2020, 1990-2020, and 2000-2020. The maps ((a), (c), and (e)) show the trends of the annual mean values across the United States. The bar plots ((b), (d), and (f)) show the fraction of sites for trends in monthly mean, annual mean, annual high7dmax, and annual low7dmin temperatures. The barplots and maps are coloured based on the seven likelihood categories (Likely: $p_i \leq 0.1$, Somewhat Likely: $0.33 \geq p_i > 0.1$. Uncertain: $0.67 \geq p_i > 0.33$, and Trend Unlikely: $0.67 > p_i$).**

220

3.2 Streamflow trends

225 Overall, the number of unique sites with any available monthly and annual mean streamflow trends data increased with more recent trend periods, with 3,321 sites in the 1980-2020 period, 3,934 sites for 1990-2020, and 4,984 sites for 2000-2020 (Hecht et al., 2024). For the three trend periods, there were 5,087, 4,973, and 5,087 unique sites with annual mean, low7d, or high7d trends data for at least one trend period, respectively.



Increasing (i.e., wetting; $p \leq 0.33$) mean annual streamflow (mean slope = +11 to +38%/decade) was two to nine times more common than decreasing (i.e., drying; $p \leq 0.33$) flow (mean slope = -14 to -23%/decade; Fig. 2), but uncertain or unlikely ($p > 0.33$) trends were the most prevalent outcome among the sites (Fig. 2). Uncertain or unlikely annual mean streamflow trends were observed at 54%, 65%, and 48% for 1980-2020, 1990-2020, and 2000-2020 trend periods, respectively.

230 Wetting trends were observed at 32%, 23%, and 48% of sites for 1980-2020, 1990-2020, and 2000-2020 trend periods, respectively. Drying trends were observed at 14%, 12%, and 4% of sites for 1980-2020, 1990-2020, and 2000-2020 trend periods, respectively.

Generally, likely trends ($p \leq 0.33$) were slightly more common with the annual mean and low7d metrics than the annual high7d metric. The annual high7d metric had increasing trends of 23%, 19%, and 38%; decreasing trends of 16%, 12%, and 9%; and uncertain or unlikely trends of 61%, 69%, and 53% for the 1980-2020 ($n=3,309$), 1990-2020 ($n=3,921$), and 2000-2020 ($n=4,971$) periods, respectively. The annual low7d metric had increasing trends of 30%, 25%, and 38%; decreasing trends of 22%, 19%, and 12%; and uncertain or unlikely trends of 48%, 56%, and 50% for the 1980-2020 ($n=3,187$), 1990-2020 ($n=3,787$), and 2000-2020 ($n=4,853$) periods, respectively.

235

Of the monthly trends, summer and spring were most representative (i.e., had a similar number of sites within each likelihood category) with their corresponding annual low7d trends and high7d trends, respectively. However, uncertain or unlikely ($p > 0.33$) monthly mean streamflow trends were the most common category across months and trend periods. Broadly, the greatest fractions of sites with likely wetting streamflow trends for the 1980-2020, 1990-2020, and 2000-2020 trend periods were winter, spring, and fall seasons months: December, January, May, and October. Generally, summer season months had the largest fraction of sites with likely drying trends, with the longer trend periods showing additional drying trends during February, March, and November. Overall, the fraction of sites with uncertain or unlikely or drying monthly mean streamflow trends tended to be greater, and the fraction of wetting trends tended to be smaller, than that of the annual trends within a given trend period, but these differences were smaller for the most recent trend period (2000-2020). For the 2000-2020 trend period, both annual mean and several monthly trends showed an even split between sites with uncertain or unlikely trends and those with wetting trends. Drying monthly streamflow was consistently the least common trend category across months and trend periods, with the most variation in site fractions across the months within a given trend period.

240

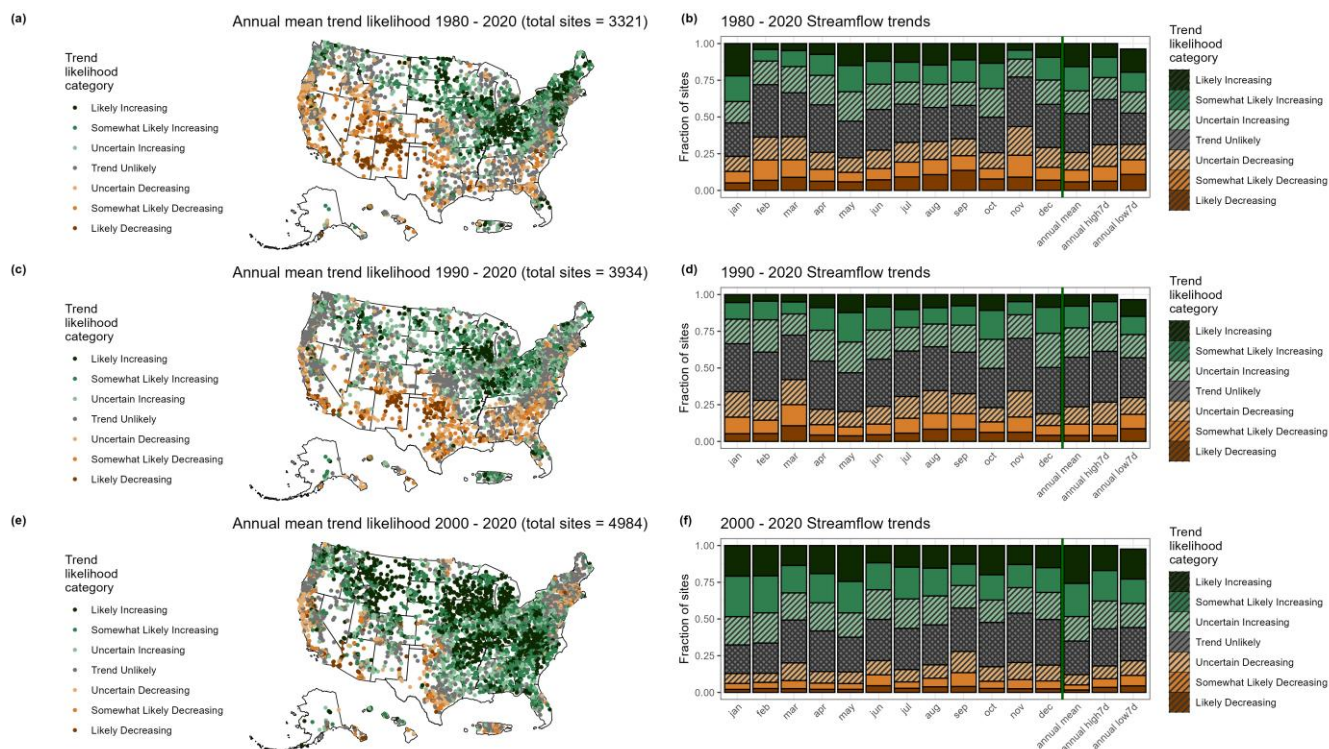
245

250

Generally, increasing annual mean trends were more prominent in the East and Midwest while decreasing trends were mostly found in the Southwest and Puerto Rico for the 2000-2020 trend period (Fig. 2(e)). Additionally, the longer trend periods had more decreasing annual mean trends across most of western and southeastern CONUS, Hawaii, and southeastern Alaska (Fig. 2(a) and 2(c)). Puerto Rico showed more increasing trends for the 1980-2020 and 1990-2020 trend periods.



255



260

Figure 2: Streamflow trends by fixed trend periods of 1980-2020, 1990-2020, and 2000-2020. The maps ((a), (c), and (e)) show the trends of the annual mean values across the United States. The bar plots ((b), (d), and (f)) show the fraction of sites for trends in monthly mean, annual mean, annual high 7-day, and annual low 7-day. The barplots and maps are coloured based on the seven likelihood categories (Likely: $p_t \leq 0.1$, Somewhat Likely: $0.33 \geq p_t > 0.1$. Uncertain: $0.67 \geq p_t > 0.33$, and Trend Unlikely: $0.67 > p_t$).

3.3 Seasonal and annual drivers of stream temperature and streamflow

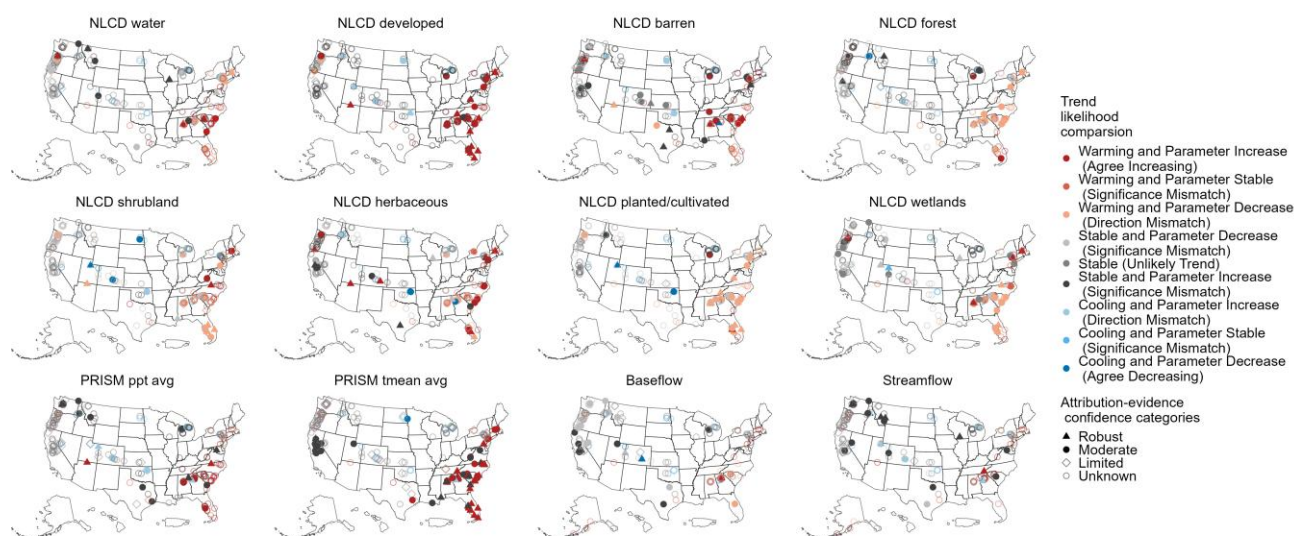
265

Trends in seasonal drivers of stream temperature and streamflow reveal potentially different influencing factors across CONUS regions. Increasing annual mean stream temperature trends for the 2000-2020 trend period correlated strongly (percentage of robust and moderate attribution-evidence sites described in Table 2) with increased air temperature (24%), decreased planted/cultivated land cover (18%), and increased developed land cover (17%). Additionally, across the Northeast, Atlantic Coast, and Florida regions (Fig. A14; hydrologic regions 1, 2, and 3) the greatest fraction of sites with robust and moderate attribution-evidence were found. For example, in these combined regions, increasing annual mean stream temperature correlated with increasing air temperature (62%) and increasing developed land cover (38%; Fig. 3). Decreased planted/cultivated (34%), wetlands (24%), forested (23%), shrublands (22%), and herbaceous (20%) land cover were correlated with increasing stream temperature along the eastern coast. However, for most of CONUS and Alaska we found much weaker correlations, where less than 10% of sites had robust or moderate driver attribution. Additionally, annual mean trends in stream temperature for the open water land cover class, precipitation, baseflow fraction, and streamflow were less correlated than the other variables for most of the CONUS and Alaska. The 1990-2020 increasing annual mean stream

270



275 temperature trends showed similar results to the 2000-2020 trend period but had a higher percentage of sites of either robust or moderate driver evidence across most of the limited sites available particularly with: increasing air temperature (49%), decreasing planted/cultivated land cover (37%), increasing developed land cover (36%), and increasing barren land cover (36%; Fig. A1).



280

Figure 3: Map of 2000-2020 annual mean stream temperature trends and attribution-evidence results by National Land Cover Database (NLCD) land cover, Parameter-elevation Regressions on Independent Slopes Model average precipitation (PRISM ppt avg) and average temperature (PRISM tmean avg), baseflow fraction (baseflow), and streamflow trends (streamflow). The colour of the points represents the comparison trend likelihood categories for stream temperature and the various drivers. The shape of the points represents the attribution-evidence categories defined in Table 2. The trend likelihood comparison categories defined as “Stable” refers to the “Unlikely” or “Uncertain” trend likelihood categories defined in row one of Table 2.

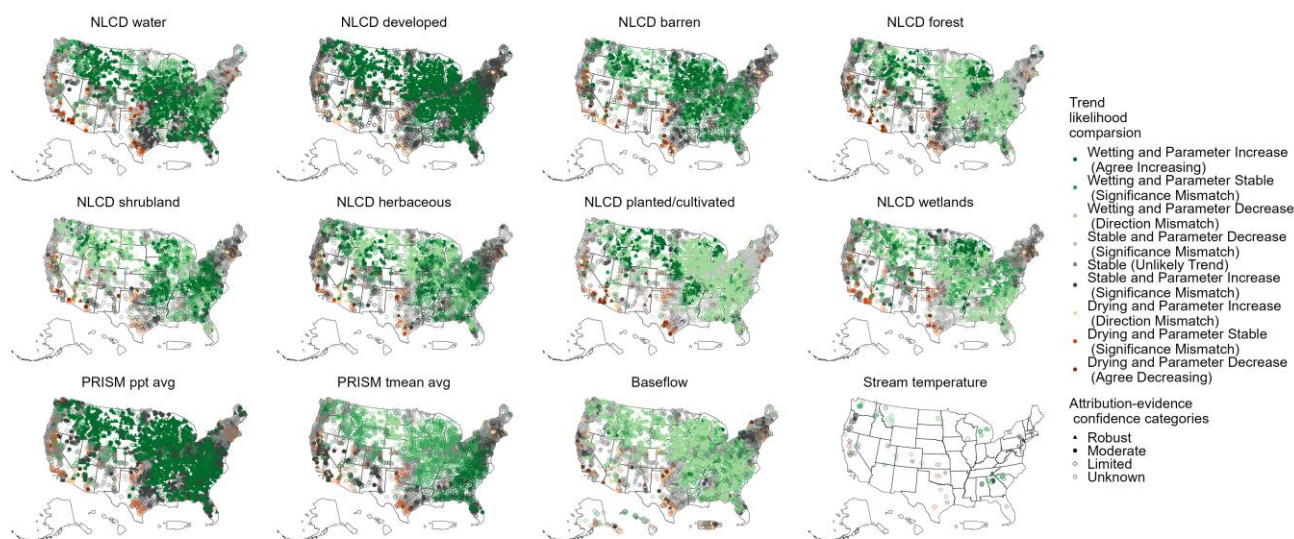
285

290 Across most of eastern, midwestern, and northern CONUS (hydrologic regions 2-7, 9-11, and 17; Fig. A14), increasing annual mean streamflow trends correlated strongly (percentage of robust and moderate attribution sites) to increased precipitation (64%), developed (45%), open water (34%), and barren land cover (30%; Fig. 4). Additionally, increasing annual mean streamflow trends were attributed to decreased baseflow fraction (45%), planted/cultivated (37%), forested (32%), and wetlands land cover (31%). Southwestern California and Arizona (hydrologic regions 16 and 18) showed decreasing annual streamflow trends that correlated with increased developed land cover (10%), decreased forested land cover (9%), and



increased air temperature (8%). Southeastern Alaska, the Island of Hawai‘i, and Puerto Rico (hydrologic regions AK, HI, and PR) showed decreasing annual streamflow with increased baseflow fraction, but the remaining Hawaiian Islands showed increasing streamflow with decreasing baseflow fraction. Decreasing annual streamflow across Texas and the southwestern CONUS (hydrologic regions 8, 12, 13, 16) during 1990-2020 correlated with increased air temperature (28%), barren land (22%), developed land (22%), and baseflow fraction (21%; Fig. A2). Additionally, decreasing annual mean streamflow trends were attributed to decreased open-water (26%) and planted/cultivated (19%; Fig. A2) land cover. Increasing annual streamflow across most of the Midwest (hydrologic regions 4 and 5) during 1990-2020 correlated with increased precipitation (50%), open water (28%), and developed land (26%), and decreased baseflow fraction (30%) and planted/cultivated land cover (25%). Puerto Rico showed increasing annual mean streamflow correlated with decreased baseflow fraction trends (7%) for the 1990-2020 trend period.

305



310

Figure 4: Map of 2000-2020 annual mean streamflow trends and attribution evidence results National Land Cover Database (NLCD) land cover, Parameter-elevation Regressions on Independent Slopes Model average precipitation (prism ppt avg) and average temperature (prism tmean avg), baseflow fraction (baseflow), and stream temperature trends (streamtemp). The colour of the points represents the comparison trend likelihood categories for stream temperature and the various drivers. The shape of the points represents the attribution-evidence confidence categories defined in Table 2. The trend likelihood comparison categories defined as “Stable” refers to the “Unlikely” or “Uncertain” trend likelihood categories defined in row one of Table 2.



Monthly stream temperature trends showed seasonal variability in the proportion of sites with moderate to robust attribution for all drivers. Seasonal trends often encompassed a larger range of moderate to robust attribution than the annual trends for each driver (Fig. 5). Trend magnitudes for stream temperature and the drivers were generally greater for monthly trends than annual trends, except for precipitation. Annual stream temperature trends most commonly had moderate to robust relationships with annual air temperature trends (40%), where most of these sites experienced increasing stream and air temperatures (34%). Monthly stream temperature trends also most commonly had strong relationships with monthly air temperature trends, led by fall (43% overall and 28% with both stream and air temperatures increasing) and followed by summer (34% and 25%), spring (30% and 17%), and winter (27% and 19%). Decreasing annual stream temperatures were most commonly related to increasing annual streamflow (10%) and decreasing baseflow fraction (7%). Decreasing monthly stream temperatures were most commonly related with decreasing air temperatures in fall (13%) and increasing streamflow in spring (12%) and summer (11%). Stream temperature trends during 1980-2020 (Fig. A3) and 1990-2020 (Fig. A4) showed similar patterns as the 2000-2020 trends. In addition, the longer trend periods showed more moderate to robust correlations with increasing stream temperature and increasing air temperature, though available sites were concentrated in the East Coast and upper western U.S. regions for these trend periods.

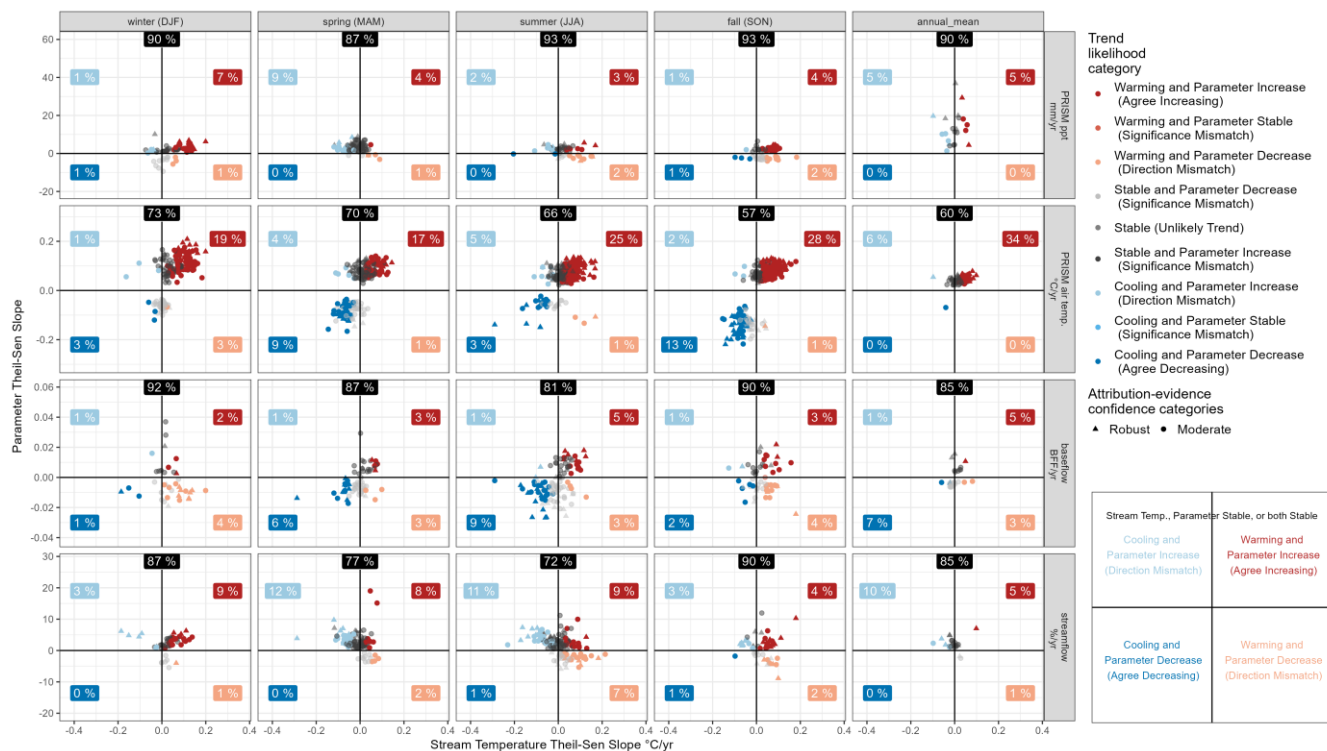
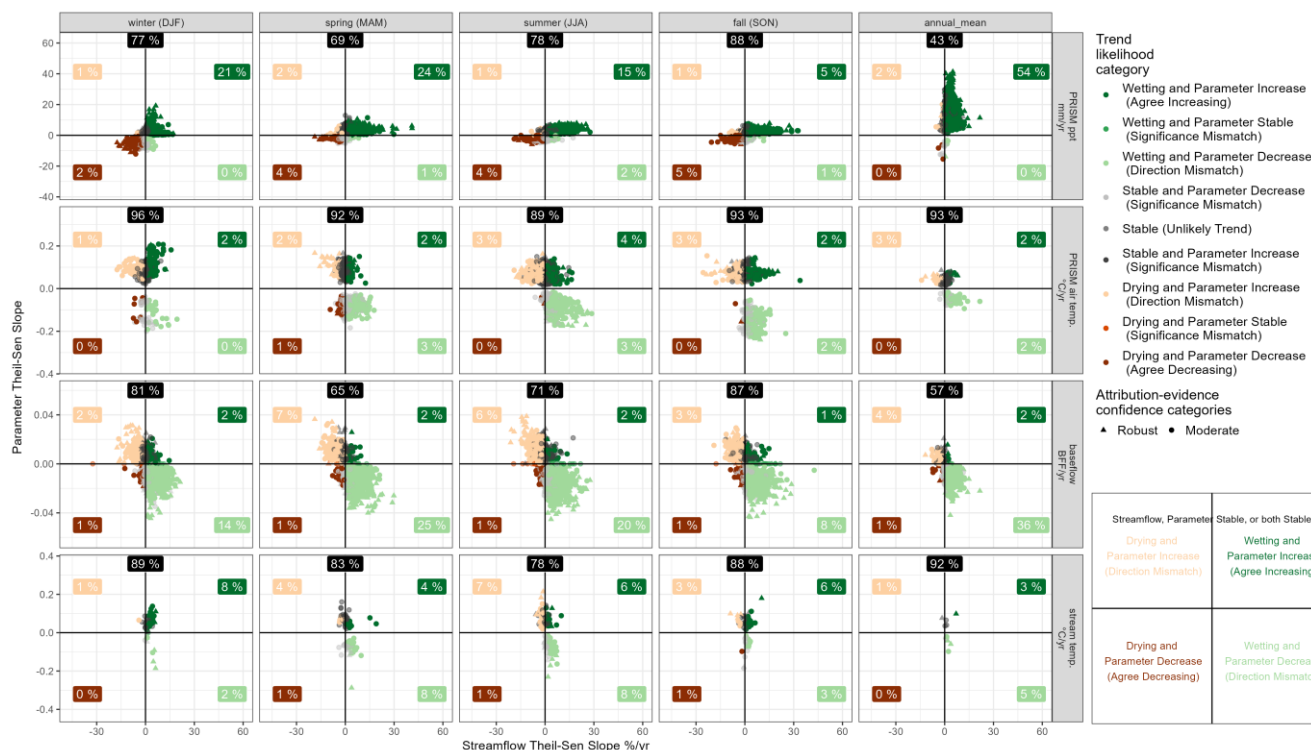


Figure 5: Seasonal stream temperature trends for 2000-2020 and attribution evidence results by climate, baseflow, and streamflow drivers. Winter = December, January, and February (DJF), Spring = March, April, and May (MAM), Summer = June, July, and August (JJA), and Fall = September, October and November (SON). The location of the points represents the monthly or annual Theil-Sen slope values for stream temperature in degrees Celsius per year plotted against potential attribution parameters of PRISM precipitation (PRISM ppt) in millimetres per year, PRISM average air temperature (PRISM air temp) in degrees Celsius per year, baseflow (BFF/yr) in millimetres per year, and streamflow (%/yr) in percent per year.



335 **baseflow fraction (BFF) per year, and streamflow in percent change per year. For example, one site may have as many as three**
monthly data points represented in one seasonal facet. The colour of the points represents the comparison trend likelihood categories
for stream temperature and the various drivers. The shape of the points represents the attribution-evidence categories defined in
Table 2. The trend likelihood comparison categories defined as “Stable” refers to the “Unlikely” or “Uncertain” trend likelihood
categories defined in row one of Table 2. Each quadrant includes the total percentage of sites that are defined as having “Robust”
340 or “Moderate” evidence, and the top middle percentage is the total percentage of sites that are defined as “Limited” or “Unknown”
evidence. The “Limited” and “Unknown” points were removed from the plots for clarity; Fig. A5 includes these points. Percentages
may not total 100 due to rounding.

Annual 2000-2020 streamflow trends showed more moderate to robust relationships with precipitation (56%) and
baseflow fraction (43%) drivers than monthly trends, while monthly streamflow trends showed slightly more relationships
345 with stream temperature (11-22%), and both showed relatively few examples of moderate to robust relationships with air
temperature (4-11%) (Fig. 6). Most sites (65-96%) showed limited or unknown attribution evidence between monthly
streamflow and the drivers. Annual precipitation trends showed greater magnitudes than the monthly trends because these are
summed metrics, where the annual precipitation trend slope is larger in magnitude than the monthly metrics. Annual increasing
streamflow trends were most commonly associated with increasing precipitation (54%) and decreasing baseflow fraction
350 (36%). Increasing monthly streamflow was most commonly moderately to robustly correlated with increasing precipitation in
spring (24%), followed by winter (21%), summer (15%), and fall (5%). Subsequently, most sites (54%) showed moderate to
robust evidence of increasing annual streamflow correlated with increasing annual precipitation. Increasing streamflow was
most commonly correlated with decreasing baseflow fraction in the spring (25%) and summer (20%), and less commonly in
the winter (14%) and fall (8%). Decreasing streamflow was most commonly correlated with increasing baseflow fraction in
355 the spring (7%) and summer (6%), and stream temperature in the summer (7%). Streamflow trends from 1980-2020 and 1990-
2020 were similar to the 2000-2020 trends displayed in Figure 6. However, decreasing streamflow with increasing baseflow
fraction relationship was more common across all seasons, as well as increasing summer air temperature (Fig. A6 and A7).

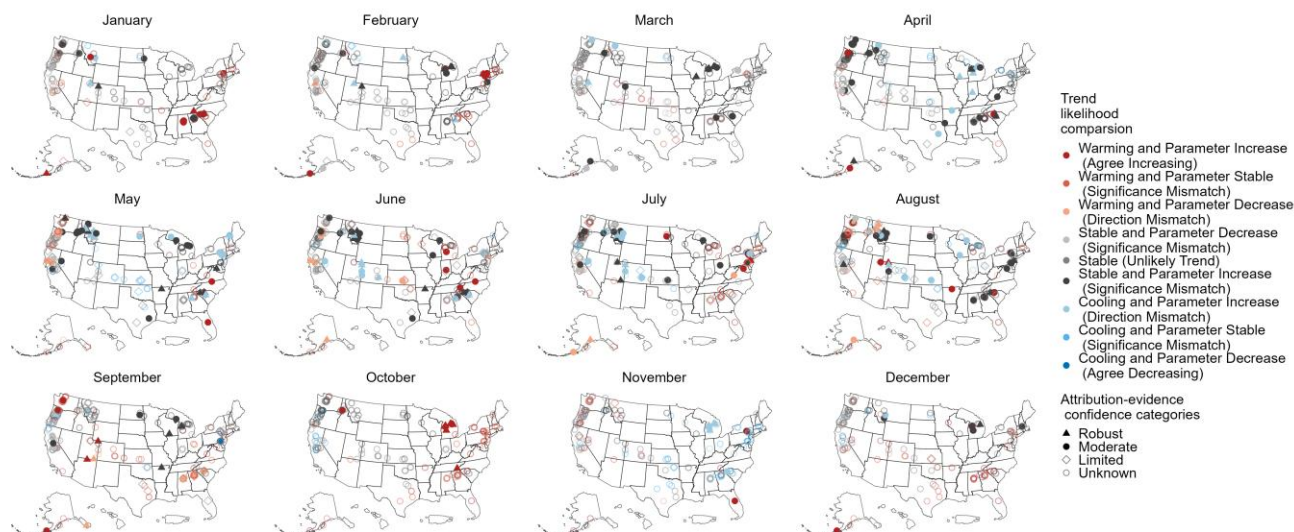


360 **Figure 6: Seasonal streamflow trends for 2000-2020 and attribution evidence results by climate, baseflow, and streamflow drivers.**
 Winter = December, January, and February (DJF), Spring = March, April, and May (MAM), Summer = June, July, and August (JJA), and Fall = September, October and November (SON). The location of the points represents the monthly or annual Theil-Sen slope values for stream temperature in degrees Celsius per year plotted against potential attribution parameters of PRISM precipitation (PRISM ppt) in millimetres per year, PRISM average air temperature (PRISM air temp) in degrees Celsius per year, baseflow fraction (BFF) per year, and stream temperature in degrees Celsius per year. For example, one site may have as many as three monthly data points represented in one seasonal facet. The colour of the points represents the comparison trend likelihood categories for stream temperature and the various drivers. The shape of the points represents the attribution-evidence categories defined in Table 2. The trend likelihood comparison categories defined as “Stable” refers to the “Unlikely” or “Uncertain” trend likelihood categories defined in row one of Table 2. Each quadrant includes the total percentage of sites that are defined as having “Robust” or “Moderate” evidence, and the top middle percentage is the total percentage of sites that are defined as “Limited” or “Unknown” evidence. The “Limited” and “Unknown” points were removed from the plots for clarity; Fig. A8 includes these points. Percentages may not total 100 due to rounding.

375 Monthly stream temperature and streamflow show both cohering and differing trends for sites where both measurements were available (Fig. 7; a total of 218 sites). Sites with decreasing stream temperature and increasing streamflow trends with robust or moderate attribution were most prevalent in April across the Great Lakes and Midwest (10 sites; hydrologic regions 4 and 5), in May for the northern latitudes of CONUS (13 sites; hydrologic regions 1, 4, 9, 10, and 14), and in June, July, and August across the Rocky Mountains and Great Lakes (12 sites; hydrologic regions 4, 14, and 15). Sites with increasing stream temperature and decreasing streamflow trends with robust or moderate attributions were most prevalent in May, June, and August in the Pacific Northwest (8 sites; hydrologic region 17), in June, July, and August for Alaska (2 sites; hydrologic region AK), and in September for the southeastern CONUS (4 sites; hydrologic regions 2, 6, 7, and 8). Sites with increasing stream temperature and increasing streamflow trends with robust or moderate attribution were most prevalent in



January and October in the eastern CONUS (20 sites; hydrologic regions 1, 2, 4, 6, and 8), and in September in the Central Rockies and Pacific Northwest (4 sites; hydrologic regions 15 and 17).



385 **Figure 7: Map of 2000-2020 monthly mean stream temperature trends and attribution evidence results by streamflow trends (s total of 218 sites). The colour of the points represents the comparison trend likelihood categories for stream temperature and streamflow. The shape of the points represents the attribution-evidence categories defined in Table 2. The trend likelihood comparison categories defined as “Stable” refers to the “Unlikely” or “Uncertain” trend likelihood categories defined in row one of Table 2.**

3.4 Hydrologic region trends

390 We selected three hydrologic regions to highlight areas of CONUS where streamflow was increasing or decreasing across the region and where there was consistent stream temperature monitoring across all trend periods (Fig. 1 and 2). The Midwest hydrologic region exhibited increasing annual streamflow across all trend periods (Fig. 2). Generally, streamflow trends were related to increasing precipitation and decreasing baseflow fraction at a similar percentage of sites from 2000-2020 across all seasons. Overall, seasonal trends and their relationship with drivers were congruent with the annual results for
 395 the Midwest hydrologic region. However, in the fall, decreasing streamflow resulted in a smaller number of sites correlated to decreasing precipitation (5%) and increasing baseflow fraction (2%; Fig. A9).

The California-Nevada hydrologic region presented seasonal complexity and dissonance with annual trends and driver correlates. The California-Nevada hydrologic region mostly showed unlikely or uncertain trends but decreasing



streamflow trends were also prominent in this region across all trend periods (Fig. 2). Decreasing winter streamflow trends
400 during 2000-2020 showed robust or moderate correlation with decreasing precipitation (10%), increasing air temperature (8%),
and increasing baseflow fraction (7%; Fig. A10). In the spring, declining streamflow during 2000-2020 correlated similarly
with decreasing precipitation (3%) and increasing air temperature (5%) but was more strongly correlated with increasing
baseflow fraction (22%). Sites with decreasing streamflow in the fall were poorly correlated with precipitation (0%) and
slightly more correlated with increasing air temperature (6%) and increasing baseflow fraction (4%). Conversely, sites with
405 increasing fall streamflow were correlated with decreasing baseflow fraction (8%). The annual decreasing streamflow trends
were correlated with increasing air temperatures (26%) and annual increasing streamflow trend sites are more correlated with
decreasing baseflow fraction (26%). Correlation between stream temperature and streamflow trends was strongest in the
summer for sites with both decreasing streamflow and decreasing stream temperature (6%).

The Atlantic Coast hydrologic region had the most stream temperature gages across all trend periods, and the results
410 illustrate the complexity of seasonal trends underlying annual trends (Fig. 1). Annual trends in stream temperature during
2000-2020 were strongly correlated with increasing air temperature (90%) and less correlated with increasing precipitation
and increasing baseflow fraction (Fig. A11). Unpacking seasonal trends in stream temperature showed that rising winter stream
temperatures correlated with increasing precipitation (21%), increasing air temperature (46%), and increasing streamflow
(17%). Spring and summer stream temperatures showed an increasing trend that was correlated with increasing air temperature
415 (18% and 32%, respectively) and increasing streamflow (17% and 16%, respectively). In contrast, fall exhibited stream
temperature increases that were correlated with increasing precipitation (6%), air temperature (59%), and baseflow fraction
(12%). In addition, decreasing stream temperature in the fall was more correlated with decreasing air temperature (29%).
Overall, in the Atlantic Coast region, trends had contradicting results across seasons that likely reduced the strength of the
annual trend.

420 The regional climate influence (PRISM annual mean air temperature and precipitation) in the starting (1980, 1990,
and 2000) and ending (2020) years of each trend period on streamflow and stream temperature trends was significant (p -value
< 0.001) across most starting years and hydrologic regions (Fig. A12 and A13). For the Midwest region, 1990 precipitation
was higher than the other years, with 2020 slightly higher than 1980 and 2000, which can lead to general bias toward negative
streamflow trends in the 1990-2020 trend period and bias toward positive streamflow trends in 1980-2020 and 2000-2020
425 trend periods. The air temperatures in 1990 and 2020 were higher than in the other years, which can lead to positive bias in
stream temperature trends for 1980-2020 and 2000-2020 trend periods and more neutral bias in trends for the 1990-2020 trend
period. For the California-Nevada region, 2020 precipitation was slightly lower than the starting trend period years, which
could lead to more negatively biased streamflow trends, with potentially steeper streamflow Thiel-Sen slopes in 1980-2020
than 1990-2020 and 2000-2020 trend periods. The air temperature between the starting trend period years and 2020 did not
430 show much of an observable difference and may be more biased toward unlikely or uncertain trends. The Atlantic Coast region
2020 precipitation was much higher than the starting trend period years and could lead to positively biased streamflow trends.
Like the Midwest region, the air temperature in 1990 and 2020, was higher than the other years, which could lead to positively



biased stream temperature trends for 1980-2020 and 2000-2020 trend periods and less bias in trends for the 1990-2020 trend period. Refer to Fig. A12 and A13 for additional information on the regional climate influence across all hydrologic regions.

435 4 Discussion

This study provides a unique assessment of contemporaneous trends in streamflow and stream temperature across the US, providing novel insight into (1) broad spatial patterns and dependencies in trends, (2) level of agreement between annual and monthly trends, (3) regional factors acting as potential drivers of trends, (4) comparison between trend periods, and (5) challenges and opportunities for trend assessment and interpretation.

440 4.1 Annual stream temperatures are getting warmer across the U.S.

Stream temperatures in the U.S. have been generally increasing more often than decreasing across different seasons, regions, and trend periods, given the relative spatial bias in the sample location distribution. Our findings concur with the CONUS results of Kelleher et al. (2021) for similar 20- and 40-year trend periods, and over trend periods from 24 to nearly 100 years in length by Kaushal et al. (2010). During the most recent 21-year trend period (2000-2020), both stream and air 445 temperatures showed warming trends, aligning with the observations of Kelleher et al. (2021). However, monthly mean stream temperature trends were predominantly uncertain or unlikely ($p > 0.33$), with the weakest warming or even cooling trends observed in November.

Monthly stream temperature trends were more variable than annual trends, with summer months exhibiting the highest magnitude of warming trends and influencing annual mean results. Summer monthly trends correlated strongly with annual 450 mean and high7dmax trends, while winter monthly trends correlated strongly with annual low7dmin trends. The prevalence of warming trends was highest in summer, October, and winter months, while shoulder season months (February-April, November) had the lowest fractions of sites with likely ($p < 0.1$) warming mean temperature trends. Notably, November trends often deviated from other months, having greater uncertain to unlikely and cooling trends. Therefore, changes in stream temperatures are not uniform throughout the year, with uncertain or unlikely monthly trends being most common and least 455 variable between trend periods and cooling less common and more variable than warming trends. Differences in prevalence of these monthly trend categories versus the annual trends were smallest for the most recent trend period (2000-2020) but generally showed greater prevalence of uncertain, unlikely, and cooling monthly trends than the annual trends and less warming prevalence. Although annual mean temperatures generally warmed, annual high7dmax and low7dmin were often uncertain to unlikely, with annual high7dmax more likely to show cooling trends. Evaluating multiple aspects of the stream thermal regime 460 is crucial for a comprehensive understanding of long-term changes and their potential drivers.

Because of the limited number of sites with long-term continuous stream temperature data, assessing regional patterns was difficult, especially for the 1980-2020 and 1990-2020 trend periods. However, some general patterns emerged. From the longest (1980-2020) to the shortest (2000-2020) trend period, a few regions within central CONUS exhibited an increase in



the fraction of sites experiencing cooling annual mean trends (i.e., hydrologic regions 9, 12, and 15). Conversely, regions
465 across western CONUS exhibited an increase in the fraction of sites with uncertain or unlikely trends (i.e., hydrologic regions
14, 17, and 18). Eastern regions showed relatively consistent high fractions of sites with warming trends (i.e., hydrologic
regions 2 and 6). For the Atlantic Coast sites, warming air temperature and increasing developed land-use trends likely drove
many of the warming stream temperature trends based on correlation coefficients reported here (Figs. 1, 3). The Northeast
region had a similar number of sites with either uncertain, unlikely, or warming trends across the three trend periods. We found
470 warming air temperature to be highly correlated with these sites, consistent with the 31-year period (1979-2009) study in
Oregon by Arismendi et al. (2013) that showed stream temperature warming was common, but more frequent for minimum
temperatures compared to maximum temperatures, and the greatest stream temperature warming occurred during the winter.
Similarly to Kelleher et al. (2021), the greatest frequency of cooling stream temperatures in California were in the late fall and
early winter (October, November, December), which is a divergence from the broad, annual warming trend across western
475 CONUS.

Increases in developed land cover and air temperatures were the primary drivers of increasing stream temperature for
many monitoring locations, especially within the Atlantic Coast region. Land cover shifts from natural vegetation to developed
land use have been a well-documented factor in stream temperature increases in previous studies (e.g., LeBlanc et al., 1997;
Nelson and Palmer, 2007; Horne and Hubbart, 2020). In other cases, stream temperature increases have been associated with
480 air temperature increases related with “heat island” effects, a phenomenon in developed areas where temperatures are relatively
warmer than the nearby rural areas (e.g., Kaushal et al., 2010; Somers et al., 2013; Zahn et al., 2021). When air temperature
increases, larger watersheds can experience greater stream temperature increases because of increasing contact time between
air and water (Rice and Jastram, 2015; Segura et al., 2015).

Stream temperature trends can be compounded by changes in streamflow, which are also moderated or amplified by
485 land use trends. For example, increases in streamflow can obscure stream temperature increases, or even cause decreasing
stream temperatures (Isaak et al., 2012; Woltemade and Hawkins, 2016; Sun et al., 2015; Webb et al., 2003; Mayer, 2012),
especially if baseflow fractions increase. In this study, we found that spring and summer streamflow were most commonly
correlated with stream temperature, which could highlight how increased streamflows are muting the signal of warming
temperatures. Conversely, in the late summer and fall, air temperature was correlated with stream temperature, when
490 streamflow is typically at its lowest point and has less of an impact on stream temperature. Therefore, seasonal shifts in
dominant drivers of stream temperatures are likely occurring in many areas of the U.S.

4.2 A recent shift towards rising streamflow in the U.S. amid long-term stability?

4.2.1 Annual mean streamflow trends

We found increases in streamflow were more frequent than streamflow declines across seasons and most geographic
495 areas in CONUS during the most recent trend period (2000-2020). Annual increasing streamflow trends in the Upper



Mississippi (hydrologic regions 4 and 5), Missouri (hydrologic regions 10 and 11), and Ohio River (hydrologic regions 5 and 6) basins were similar to prior results (Sagarika et al., 2014; Kalra et al., 2008; Ayers et al., 2019; Tamaddun et al., 2016). In some regions, recent streamflow increases represent a change in trend direction from earlier trend periods. For example, the longstanding decreasing streamflow trend in southeastern CONUS (our 1980-2020 and 1990-2020 trend periods; also refer to 500 Wilbanks et al., 2025; Tamaddun et al., 2016; Lins and Slack, 1999) shifting to an increasing streamflow trend during the 2000-2020 trend period could be critical in this region, which has experienced increasing water demand (Brown et al., 2019) and stresses on water availability in recent decades (Sun et al., 2008). Prior work has shown generally decreasing annual mean streamflow trends in the Pacific Northwest (Kalra et al., 2008; Lins and Slack, 1999; Sagarika et al., 2014; Tamaddun et al., 2016). Our work, in contrast, shows annual mean streamflow trends switching from primarily uncertain or unlikely (1980- 505 2020 and 1990-2020) to increasing streamflow trends for 2000-2020, which could help alleviate current stresses on water supply and anadromous fish (Mote et al., 2003; Wu et al., 2012). A final example of a recent reversal or change of longstanding decreasing streamflow trends is the State of Hawaii (trend period 1987-2016 as shown in Clilverd et al, 2019): our work indicates a recent switch (2000-2020 trend period) to increasing annual mean streamflow and decreasing baseflow fraction. Hawaii shows large within-region variability, however, with decreasing streamflow and increasing baseflow fraction for the 510 Island of Hawai'i (2000-2020 trend period), confirming prior results by Bassiouni and Oki (2013). Not all U.S. regions experienced increasing streamflow during the recent 2000-2020 trend period. For example, southeastern Alaska showed decreasing annual mean streamflow and increasing baseflow fraction for the 2000-2020 trend period, indicating a potential decreasing shift in a precipitation-dominated region of Alaska (Curran and Biles, 2021). We also found regional annual decreasing streamflow trends across all trend periods in the southwestern CONUS, similar to results by Ficklin et al. (2016). 515 Puerto Rico showed decreasing annual mean streamflow for the 2000-2020 trend period, consistent with climate model projections that the island will experience more drying in future scenarios (Taylor et al., 2018), although longer term trends from 1990-2020 show increasing streamflow. Changing streamflow trend directions depending on the trend period, as shown here for multiple regions of the U.S., could complicate decadal water resources planning and management efforts.

Studies of streamflow trends tend to focus on significant increases and decreases; however, uncertain or unlikely 520 trends ($p > 0.33$) were the most common streamflow trends (>50% of sites) found herein across all the trend periods except 2000-2020. Prior work on CONUS annual streamflow trends showed broadly increasing streamflow over trend periods prior to 2000 (Lins and Slack, 1999; McCabe and Wolock, 2002; Rice et al., 2015). Further examination of the results from prior work, however, shows that “no trend” or “uncertain” trends in streamflow are a common, but less emphasized, result across CONUS. For example, in Lins and Slack (1999), at the 50% percentile of annual daily discharge only 25-46% of sites (their 525 Table 1, depending on the trend period) had a significant trend, indicating that most CONUS sites had no or uncertain streamflow trend. McCabe and Wolock (2002) showed that over half of CONUS sites had increasing median daily streamflow in selected trend periods from 1941 through 1999, but predominantly for trend periods prior to 1970 with uncertain or no trend being the most prevalent result after 1970 (refer to Fig. 2B in McCabe and Wolock, 2002). In the context of water supply, uncertain or unlikely streamflow trends can be a key indicator in water availability assessments for CONUS (Stets et al., 2025),



530 highlighting the potential importance of streamflow being largely stable within the bounds of trend detection uncertainty over the trend periods 1980-2020 and 1990-2020 in many regions across CONUS.

4.2.2 Monthly and seasonal streamflow trends

We found that seasonal trends may be offset or masked by other opposing seasonal trends when analysed annually. Annual low- and high-flow metric trends tend to indicate monthly mean trends during the lowest (summer) and highest (winter and spring) magnitudes of the annual hydrograph, respectively. Generally, the annual mean, low7d, and high7d had the greatest fraction of sites with wetting, drying, and uncertain or unlikely ($p > 0.33$) trends, respectively. Sub-annual trends, potentially masked at the annual timescale, can be critical for water resources management (Singh and Basu, 2022), water quality (Murphy and Sprague, 2019), and ecological flows (Davies et al., 2014). Relatively few studies, however, have examined seasonal streamflow trends in the U.S. (Lettenmaier et al., 1994; Sagarika et al., 2014; Singh and Basu, 2022). Seasonal trends also vary by the trend period examined; the 1980-2020 trend period has more decreasing streamflow trends across all months relative to the 1990-2020 and 2000-2020 trend periods. The dependence of the estimated trend on the trend period examined is a known challenge, and we attempted to assess this by comparing climate metrics between the starting years and ending year (Figs. A12 and A13; DeGaetano, 2009; Dudley et al., 2017; Huh et al., 2005).

Seasonal and monthly trends provide deeper insight than annual trends alone into potential drivers of streamflow shifts. For example, increasing streamflow trends in winter and spring were correlated with increasing precipitation trends in those seasons, whereas decreasing baseflow fraction trends were correlated across all seasons with increasing streamflow trends and therefore may have a more substantial influence on annual trends. Prior work has shown that seasonal precipitation trends are a strong driver of seasonal streamflow trends and that regional differences in seasonal precipitation trends can determine regional streamflow trends (Ficklin et al., 2016; Singh and Basu, 2022). Additionally, baseflow fraction during the spring appears to show a stronger negative correlation with streamflow, than other seasons and annually, an indication of increased precipitation or snowmelt likely influencing runoff and the decreased reliance of baseflow fraction across the 2000-2020 trend period (Ficklin et al., 2016). Alternatively, southern CONUS for the 1990-2020 trend period shows most sites have increasing baseflow fraction and decreasing streamflow, an indication of increased dependence on groundwater in these locations (Fig. A6; Ayers et al., 2022). Seasonal air temperature trends are also shown here to influence seasonal streamflow trends in certain regions, particularly those that have numerous snow-dominated watersheds, such as the Upper Missouri River Basin (hydrologic regions 10 and 11); the sensitivity of streamflow in this region to increasing air temperatures has also been highlighted by Wise et al. (2018) and Martin et al. (2020). Alignment between precipitation trends, developed land cover, and air temperature trends can amplify increasing seasonal streamflow trends (e.g., warming air temperatures coupled with precipitation increases combined with land-cover-driven streamflow shifts), as shown here for the eastern, midwestern, and northern CONUS (Fig. 4 for 2000-2020, Fig. A2 for 1990-2020), and shown previously by Dudley et al. (2017) and Kelly et al. (2017). Opposing directional trends, such as increasing air temperature and decreasing precipitation may also magnify streamflow decreasing trends, shown here for the Atlantic Coast, Texas, and the southwestern regions for 1990-2020 (Fig.



565 A2). Previous studies have shown the same synergistic driver interactions to intensify regional decreasing streamflow trends. For example, Wilbanks et al. (2025) showed the amplification of decreasing streamflow trends in the southeastern U.S. through a combination of decreasing precipitation, increasing water use, and increasing air temperature.

4.3 Alignment and dissonance between streamflow and stream temperature

570 Across the United States, most sites had uncertain or unlikely ($p > 0.33$) trends for the annual metrics, seasons, and trend periods for both streamflow and stream temperature. This was followed by increasing trends, while the smallest percentage of sites had decreasing trends. There were variations in the fraction of sites, the magnitude of trends, and the correlation with drivers between annual metrics and monthly mean metrics across all seasons. Annual trends were smaller than seasonal trends for stream temperature (similar to Kelleher et al., 2021), streamflow, air temperature, and baseflow fraction (Fig. 6).

575 There was notable coupling between streamflow trends and stream temperature trends. During spring and summer, warming stream temperatures correlated with decreasing streamflow, while cooling stream temperatures correlated with increasing streamflow (Fig. 5). The mountainous regions in the northern latitudes within CONUS in May, and the central Rocky Mountains in June and July, showed cooling stream temperature trends with wetting streamflow trends (Fig. 7). This indicates a possible shift in snowmelt timing affecting late spring to early summer stream temperature and streamflow in snow-dominated regions (Ford et al., 2021; Uzun et al., 2021; Dudley et al., 2017). In the arid regions of southwestern CONUS, 580 decreasing streamflow was linked to increasing air temperatures and, to a lesser degree, increasing stream temperatures (Fig. A2, A3, and A4). The 1990-2020 trend period showed decreasing streamflow across the region (Fig. A2) and was correlated with increasing air temperature and decreasing precipitation, similar to findings by Xiao et al. (2018).

585 In addition, eastern CONUS showed warming and wetting trends in October, December, and January across most sites, consistent with the findings of decreasing snowpack and earlier peak flows (Ford et al., 2021), and warming streams in this region (Kelleher et al., 2021). Across a few sites in southeastern CONUS, there were warming temperatures and drying streamflows in September, which contradicts previous studies that observed wetting trends during hurricane season fall months (Fig. 7; Engström and Waylen, 2017). The results highlighted here could be a response to an extended low streamflow season attributed to increasing air temperature and decreasing precipitation during September (Simeone et al., 2024). The limited sites available in southeastern Alaska and the Alaska Peninsula (4 sites) showed warming stream temperature trends across most 590 months, which corresponded with wetting streamflow trends during the fall and winter months, but there was a drying streamflow trend during summer (June, July, and August). Increased air temperature in this region has been shown to have an important effect on streamflow and the flow regime, leading to changes in precipitation and snowmelt (Curran and Biles, 2021).



4.4 The influence of drivers was enhanced at the regional scale

595 This section focuses on three regions (Midwest – hydrologic region 5, California-Nevada – hydrologic region 18, and
Atlantic Coast – hydrologic region 2) where streamflow and stream temperature trends were identifiable and showed clearer
connections to climatic, hydroclimatic, and land-use drivers (Fig. A9, A10, and A11).

4.4.1 The Midwest hydrologic region

The Midwest hydrologic region had the greatest fraction of sites exhibiting increasing streamflow trends for the 2000-
600 2020 period. Annual and seasonal streamflow trends were predominantly increasing. Our finding that precipitation increases
were a primary driver of streamflow increases is consistent with numerous studies of streamflow trends in this region (Gupta
et al., 2018; Ayers et al., 2019; Schilling and Libra, 2003; Kelly et al., 2017; Frans et al., 2013; Xu et al., 2013). Annual
timescale increasing streamflow trends aligned with land-use trends, specifically increases in developed, barren, and water
classifications and decreases in forest, planted/cultivated, and wetlands; prior work has shown that increases in cultivated land,
605 including tile drainage, are a major driver of increasing streamflow in the Midwest (Ayers et al., 2019; Kelly et al., 2017;
Kochendorfer and Hubbart, 2010; Foufoula-Georgiou et al., 2015; Zhang and Schilling, 2006). Our analysis indicates that
recent (2000-2020) increasing streamflow trends are primarily driven by increasing precipitation and shifts in land use.

Seasonal trends in streamflow and their associated drivers in the Midwest hydrologic region indicate dampening of
seasonal streamflow trends at the annual timescale based on Theil-Sen slope magnitudes. The largest seasonal increasing
610 streamflow trend was in the fall, coincident with increasing precipitation trends and decreasing baseflow fraction trends, which
indicates that potentially more precipitation is being converted into stormflow (Melillo et al., 2014). Other studies (e.g., Ayers
et al., 2019) have shown increasing baseflow volume in the Midwest and were similarly related to changes in air temperature
that impact precipitation type, but trends were stronger in a different season (April-June).

4.4.2 The California-Nevada hydrologic region

615 The California-Nevada hydrologic region includes diverse hydroclimates ranging from high alpine environments,
irrigated agricultural valleys, and arid deserts. The region also has substantial influences upon streamflow from land-use
change (Beighley et al., 2023), climate shifts (Maurer et al., 2007), and water use (Carlisle et al., 2016). Our analysis showed
broad decreasing streamflow trends across all trend periods (Fig. 2(a), (c), (e)), consistent with prior work for the Sierra Nevada
(He et al., 2016). Streamflow trends disaggregated to smaller regions but highlighted more variability across the region, such
620 as more wetting in the Sierra Nevada range compared to drier conditions in the east (Fig. 2(a), (c), (e)). Some studies found no
significant trends in California (Sagarika et al., 2014; Kalra et al., 2008) or the Great Basin (Kalra et al., 2008). Lins and Slack
(1999) observed increasing streamflow in the Great Basin, and Rice et al. (2015) observed an even split between increasing
and decreasing streamflow trends in their Western Xeric region that included southern California and the Great Basin,
indicating that there are substantial regional variations in prior observed trends.



625 In this study, we found decreasing winter and increasing spring streamflow, which were correlated with decreasing
precipitation and decreasing baseflow fraction, respectively. As a result of more streamflow earlier in the year, our results
could indicate that wet seasons will become wetter and dry seasons will become drier in California, similar to the findings of
Mallakpour et al. (2018) and Grantham et al. (2018). On the other hand, Aguado et al. (1992) found a decreasing fraction of
total annual streamflow in April-July but increasing fractions of total annual streamflow in fall (August-October) and winter
630 (November-January) seasons in streams draining the Sierra Nevada. Prior studies have pointed out that the apparent paradox
of increasing precipitation and decreasing streamflow trends in California could be attributed to precipitation phase shifts from
snow to rain in winter months and the importance of snowmelt for sustaining streamflow throughout the summer and into fall
(Diffenbaugh et al., 2015; Li et al., 2017) because streamflow elasticity relative to precipitation can be sensitive to decreases
in the fraction of precipitation falling as snow (Hou et al., 2025). Our results showed correlations between decreasing winter
635 precipitation and decreasing winter streamflow and increasing spring precipitation and increasing streamflow (Fig. A10),
consistent with a potential shift in seasonal timing of precipitation that produces net decreasing annual streamflow trends
despite mixed seasonal streamflow trends.

In the California-Nevada region, seasonal memory, wherein prior season hydroclimatic drivers carry over into effects
onto subsequent seasons, has been shown to affect seasonal streamflow trends (Cayan et al., 2013), although we did not account
640 for seasonal memory in this study. Additional explanations for decreasing regional streamflow trends and within-region
variability are increasingly volatile swings between wet and dry extremes (Berg and Hall, 2015; Swain et al., 2018) and a
shortening of the wet season (Luković et al., 2021; Swain et al., 2021) that could affect seasonal memory and translate into
streamflow decreases.

4.4.3 The Atlantic Coast hydrologic region

645 The Atlantic Coast hydrologic region highlighted a complicated interdependence between stream temperature,
streamflow, and climatic trends. We found increasing fall stream temperatures that were most closely tied with increasing air
temperature. Most prior work has found either no trends (Kunkel et al., 2013; Misra et al., 2012; Pan et al., 2004; Portmann et
al., 2009) or decreasing trends in air temperature in this region (Patterson et al., 2012); However, Rice and Jastram (2015)
found an increasing monthly mean air temperature trend from 1986 to 2010. Substantial increases in stream temperatures in
650 summer and fall seasons for the middle to end of the 21st century were simulated for Atlantic Coast streams by Botero-Acosta
et al. (2022). Increasing fall streamflow trends in the region have been tied to increases in the frequency of hurricane effects
(Engström and Waylen, 2017), including increasing fall precipitation (Kunkel et al., 2013); other studies have shown annual
trends in increasing precipitation (Seager et al., 2009). In contrast, one study (Patterson et al., 2012) showed decreasing
streamflow and decreasing precipitation at the annual timescale, attributed to a change in the Atlantic Multidecadal Oscillation
655 (AMO). Wilbanks et al. (2025) also showed decreasing annual streamflow trends in the Piedmont, Southeastern Plains, and
Coast ecoregions. Our increasing 2000-2020 fall streamflow trends (Fig. 2(a), (c), (e)) point to the potential importance of
tropical cyclone effects on streamflow trends in this region (Brun and Barros, 2014; Chalise et al., 2021; Knight and Davis,



2007), in particular with respect to alleviation of drought conditions (Maxwell et al., 2012; Sun et al., 2021). Stream temperatures in the region have been shown to be increasing over recent decades (Kaushal et al., 2010), in agreement with our findings, and streamflow has also been increasing in recent decades (Rice et al., 2015). Consistent with our findings, Rice and Jastram (2015) found increasing trends in both stream temperature and streamflow, in contrast to work in other regions that has found that increased streamflow can limit stream temperature increases or even cause a stream cooling (Webb et al., 2003; Mayer, 2012). Streamflow trend analysis in the southeastern CONUS also indicates that land-use change, including changes in agricultural and forest lands (O’Driscoll et al., 2010), is affecting streamflow trends in the region (Anandhi et al., 2018), which was confirmed by our study where increased stream temperature was associated with increased developed land, decreased planted/cultivated, and decreased forested land.

4.5 Challenges and opportunities in streamflow and stream temperature trends

The trend analyses presented in this study focused on monotonic changes of streamflow and stream temperature. However, the trend analysis could be expanded upon with additional methods to detect non-monotonic changes in streams (e.g., periodic variations, teleconnections, change-points), using wavelet analysis (Rice et al., 2016) or autoregressive integrated moving averages (McCabe et al., 2023) as two example approaches. Additionally, our uncertain or unlikely trend results could be explained by non-monotonic trends that were not accounted for in this study.

The 2000-2020 trend period is only 21 years long, a relatively small sample size that reduces the statistical power of the Mann-Kendall test (Helsel et al., 2020). This reduced statistical power is especially pronounced with the stream temperature dataset that has a limited number of sites available across all trend periods. Additionally, many non-USGS stream temperature monitoring locations were not evaluated for reservoir impacts, and abrupt step changes may lead to false positive results for the Mann-Kendall trend test.

Hayhoe et. al (2007) defined “edge effects” as trend periods that include an abnormally wet or dry period at the beginning or end of the record, which can influence trend findings. We found a similar effect across most hydrologic regions in eastern CONUS, where 2020 was abnormally wet compared to the starting trend period years, and most sites in this area showed increasing streamflow trends (Fig. A12; McCabe and Wolock, 2002; Patterson et al., 2012). Air temperature edge effect influences on stream temperature were less obvious, where other drivers such as land cover may have a larger effect on stream temperature in eastern CONUS (Fig. A13; Kaushal et al., 2010). Regional differences across the variable trend periods in the annual results could also indicate the presence of longer-term temporal persistence, whereby low frequency, natural fluctuations appear as trends over certain periods (Koutsoyiannis and Montanari, 2007; Sagarika et al., 2014). Multiple trend periods were selected in this study to provide a broader view of the monotonic changes of streamflow and stream temperature across three separate starting years. Additionally, the large spatial resolution of the PRISM air temperature and precipitation datasets can cause abrupt changes between neighbouring pixels and within basins and may lead to false positive results for the



690 Mann-Kendall trend test. A more detailed analysis of edge effects and the PRISM dataset influence on streamflow and stream temperature could help inform future trend attribution studies.

Additional work would be needed to better understand the absolute spatiotemporal changes of streamflow, stream temperature, and the drivers (e.g., are colder sites getting colder, are wetter sites getting wetter). Several stream locations likely have small magnitude changes in drivers that have minimal effect on streams, and an analysis of sites with the largest seasonal
695 swings in magnitude is needed to understand the ecological and water availability effects of large changes. Kelleher et al. (2021) and Singh and Basu (2022) showed that some of the largest magnitude trends in seasonal stream temperature and streamflow were attributed to human-activity (e.g., water withdrawals, dams), and further exploration of these impacts is warranted.

The effect of spatial correlation was not accounted for in this study, where neighbouring or nested basins with similar
700 trend results potentially inflates the total count of sites when creating the bar plots in Figures 1 and 2 or calculating a percentage of sites in Figures 5 and 6. McCabe and Wolock (2002) performed a similar trend analysis without accounting for spatial correlation and acknowledged the total number of sites would be reduced but percentages of sites exhibiting significant trends would be the same.

Trends at sites may change from month-to-month (or season-to-season), and a site-specific analysis would be needed
705 to observe trends at sites changing from increasing to decreasing (or vice-versa) in adjacent months or seasons. Our study analysed the correlation of the parameters with a limited set of drivers, where a more robust analysis (e.g., regression) would be needed to determine the effect of additional drivers and statistically attribute causation on the response variable. For example, the amount of wet season in-stream baseflow received can directly influence the amount of water available in a stream during the dry season, and trends during these seasons would be important for understanding future water availability
710 (Dralle et al., 2016).

5 Conclusions

In this analysis, we (1) documented and compared decadal trends in seasonal and annual streamflow and stream temperature sites across the conterminous United States (CONUS), Alaska, Hawaii, and Puerto Rico for three trend periods (1980-2020, 1990-2020, and 2000-2020); (2) attributed trend confidence categories to determine the impact of land cover,
715 precipitation, air temperature, and baseflow fraction on streamflow and stream temperature; and (3) selected three hydrologic regions (Midwest, California-Nevada, and Atlantic Coast) within CONUS as case studies to better understand the effects of climate and land-use drivers on streamflow and stream temperature at a regional scale. Uncertain and unlikely trends were the dominant trend result for most monthly and annual metrics across all trend periods. Annual stream temperatures increased across CONUS for all trend periods. Streamflow increased across most of CONUS for the 2000-2020 period, but decreases
720 were more prominent for the 1980-2020 and 1990-2020 trend periods across southern and western CONUS. When comparing monthly results to annual trend metrics, we found the variability in the magnitude of annual trends was often smaller, which



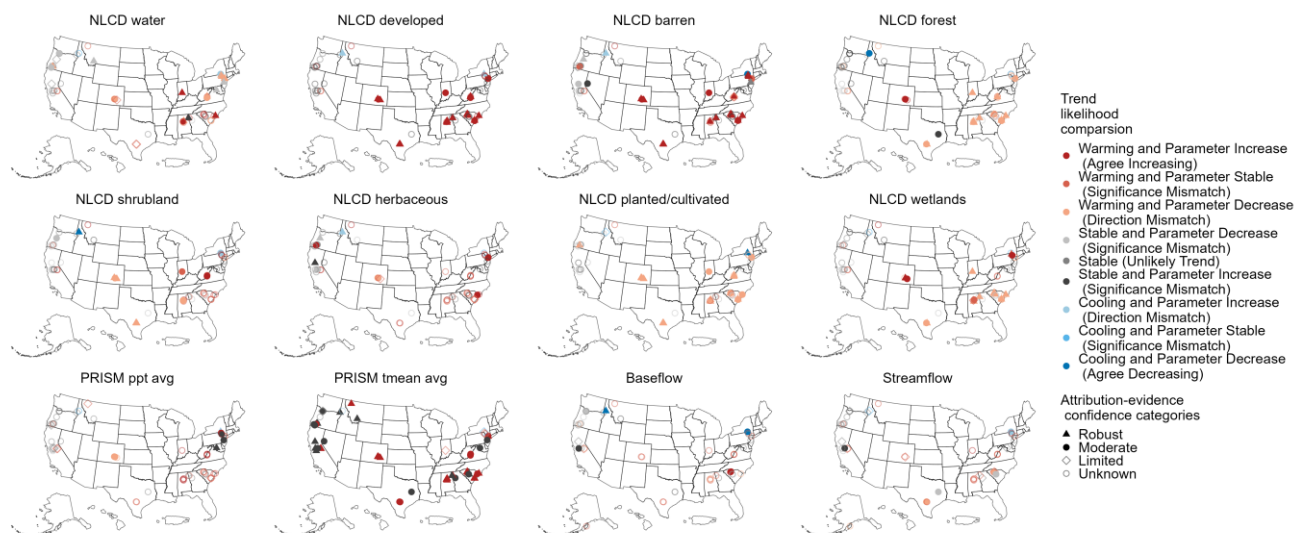
indicates important seasonally driven ecological and water resources implications may be obscured when only examining annual trends.

725 Monthly streamflow was correlated with monthly precipitation and baseflow fraction, and monthly stream temperature correlated with monthly air temperature. Increasing streamflow across most of CONUS and stream temperature in eastern CONUS was correlated with increasing developed and decreasing forested land cover. Regionally, stream temperature within the Atlantic Coast region was correlated with air temperature; streamflow within the Midwest region was correlated with precipitation in the fall and baseflow fraction in the spring; and streamflow within the California-Nevada region was correlated with baseflow fraction in the spring and summer.

730 Evaluating seasonal trends in streamflow and stream temperature, and the attribution evidence across drivers, improves our understanding of seasonal dynamics on streams and the broad effects on water resources across the U.S. Our study highlights the importance of studying streamflow and stream temperature together at large spatial scales and expanding our understanding of using monthly metrics to evaluate sub-annual impacts to streams.

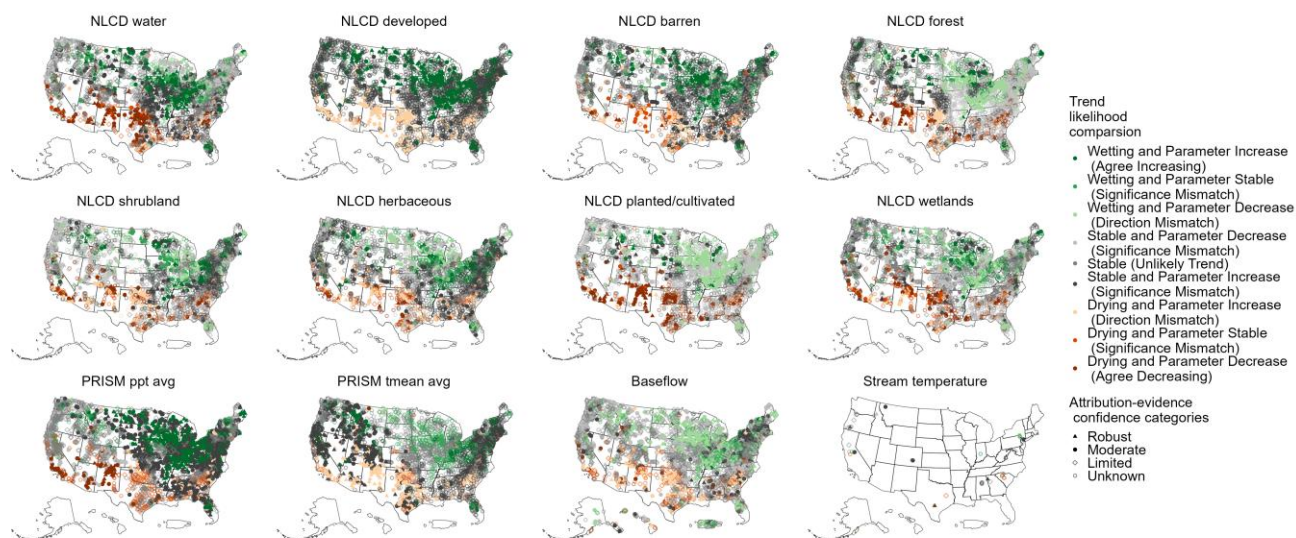


735 Appendix A



740

Fig. A1: Map of 1990-2020 annual mean stream temperature trends and attribution evidence results by National Land Cover Database (NLCD) land cover, Parameter-elevation Regressions on Independent Slopes Model average precipitation (PRISM ppt avg) and average temperature (PRISM tmean avg), baseflow fraction (baseflow), and streamflow trends (streamflow). The colour of the points represents the attribution-evidence categories for stream temperature and the various drivers. The shape of the points represents the attribution-evidence categories defined in Table 2. The trend likelihood comparison categories defined as “Stable” refers to the “Unlikely” or “Uncertain” trend likelihood categories defined in row one of Table 2.



745

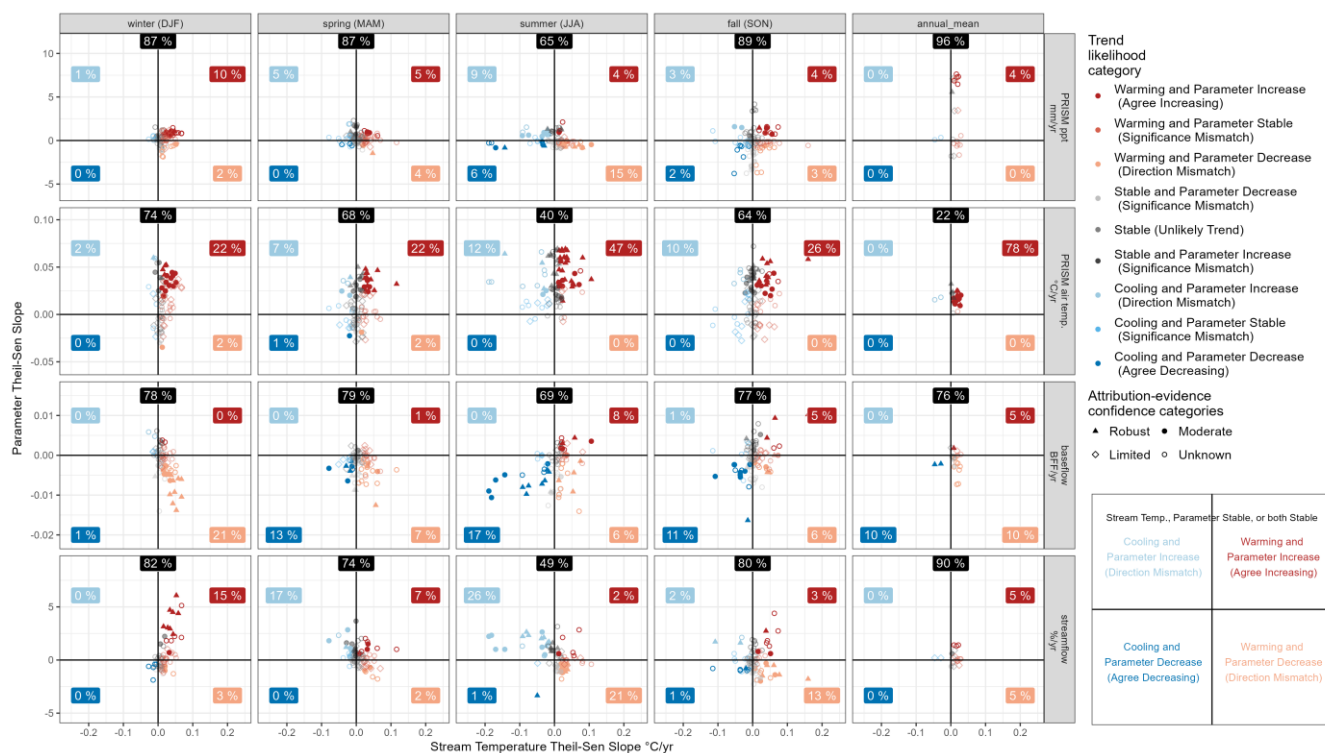
Fig. A2: Map of 1990-2020 annual mean streamflow trends and attribution evidence results by National Land Cover Database (NLCD) land cover, Parameter-elevation Regressions on Independent Slopes Model average precipitation (PRISM ppt avg) and average temperature (PRISM tmean avg), baseflow fraction (baseflow), and stream temperature trends (streamtemp). The colour of the points represents the comparison trend likelihood categories for stream temperature and the various drivers. The shape of the points represents the attribution-evidence categories defined in Table 2. The trend likelihood comparison as “Stable” refers to the “Unlikely” or “Uncertain” trend likelihood categories defined in row one of Table 2.

750

755



760



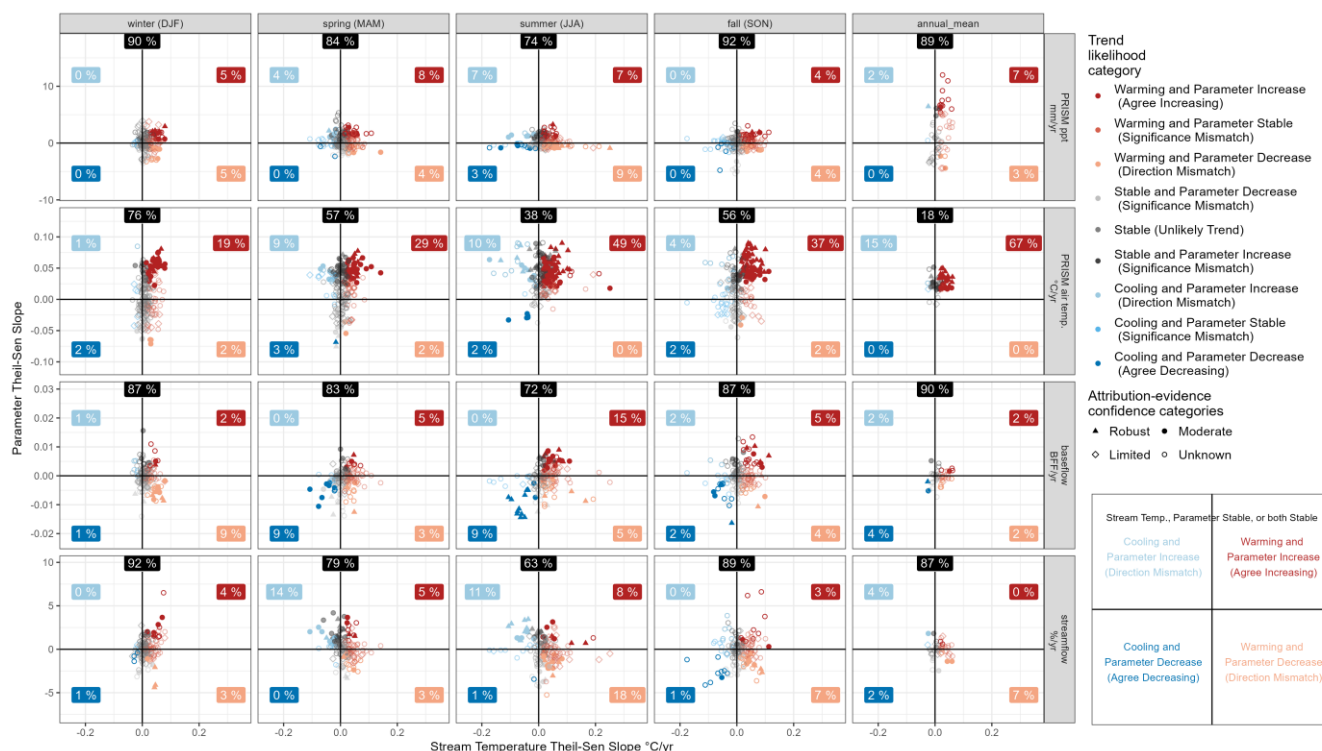
765

770

Fig. A3: Seasonal stream temperature trends for 1980-2020 and attribution evidence results by climate, baseflow, and streamflow drivers. Winter = December, January, and February (DJF), Spring = March, April, and May (MAM), Summer = June, July, and August (JJA), and Fall = September, October and November (SON). The location of the points represents the monthly or annual Theil-Sen slope values for stream temperature in degrees Celsius per year plotted against potential attribution parameters of PRISM precipitation (PRISM ppt) in millimetres per year, PRISM average air temperature (PRISM air temp) in degrees Celsius per year, baseflow fraction (BFF) per year, and streamflow in percent change per year. For example, one site may have as many as three monthly data points represented in one seasonal facet. The colour of the points represents the comparison trend likelihood categories for stream temperature and the various drivers. The shape of the points represents the attribution-evidence categories defined in Table 2. The trend likelihood comparison categories defined as “Stable” refers to the “Unlikely” or “Uncertain” trend likelihood categories defined in row one of Table 2. Each quadrant includes the total percentage of sites that are defined as having “Robust” or “Moderate” evidence, and the top middle percentage is the total percentage of sites that are defined as “Limited” or “Unknown” evidence. Percentages may not total 100 due to rounding.



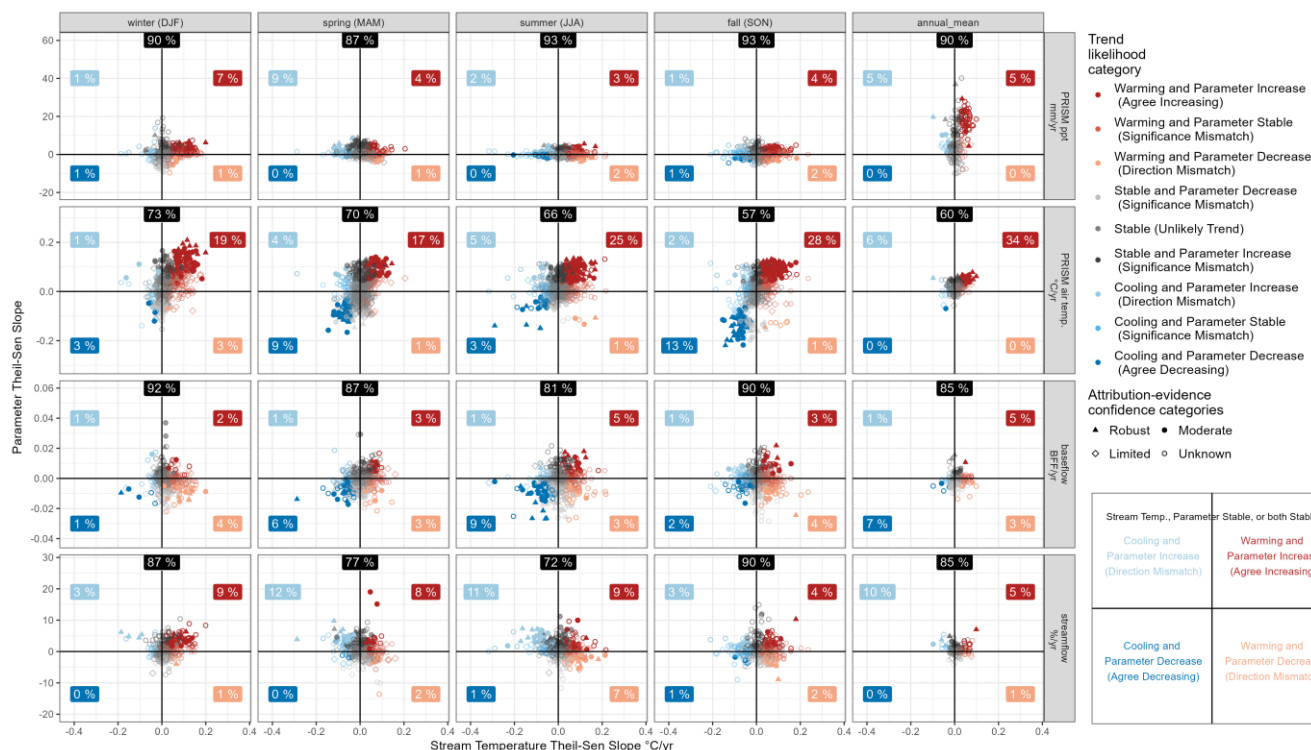
775



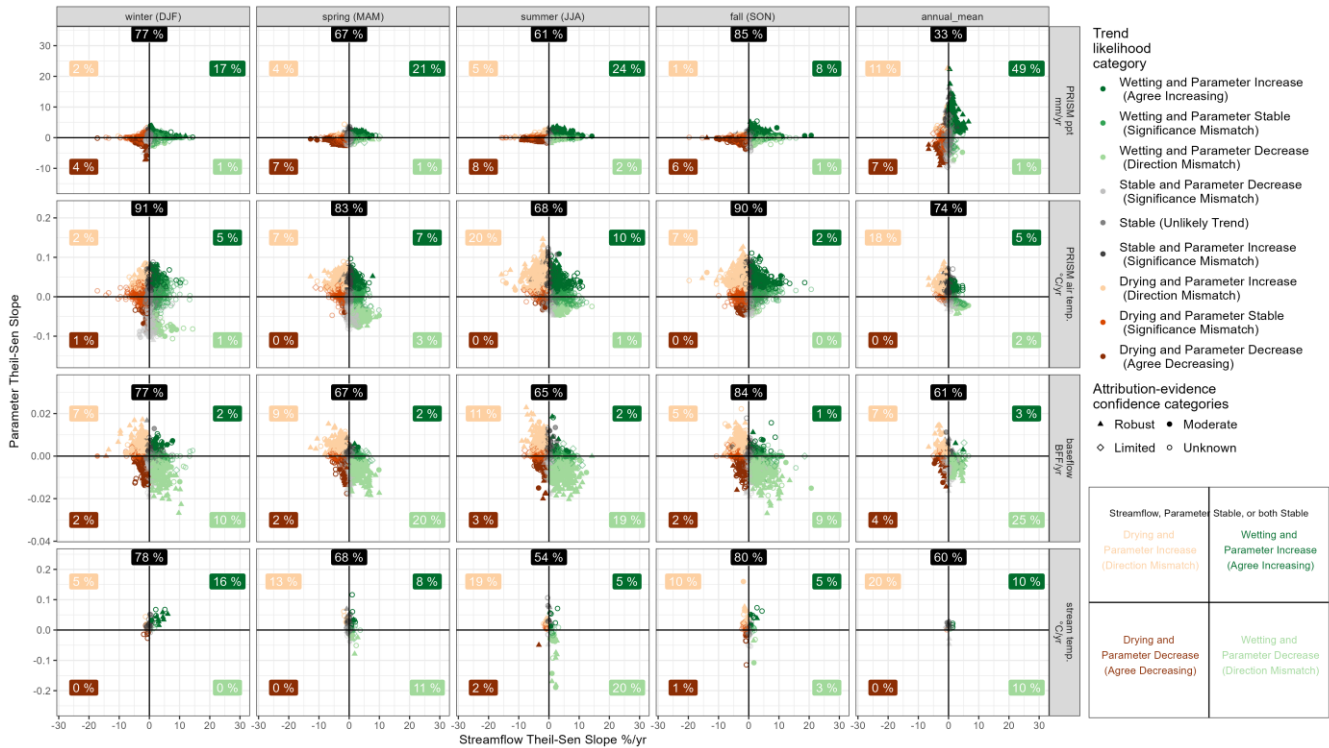
780

785

Fig. A4: Seasonal stream temperature trends for 1990-2020 and attribution evidence results by climate, baseflow, and streamflow drivers. Winter = December, January, and February (DJF), Spring = March, April, and May (MAM), Summer = June, July, and August (JJA), and Fall = September, October and November (SON). The location of the points represents the monthly or annual Theil-Sen slope values for stream temperature in degrees Celsius per year plotted against potential attribution parameters of PRISM precipitation (PRISM ppt) in millimetres per year, PRISM average air temperature (PRISM air temp) in degrees Celsius per year, baseflow fraction (BFF) per year, and streamflow in percent change per year. For example, one site may have as many as three monthly data points represented in one seasonal facet. The colour of the points represents the comparison trend likelihood categories for stream temperature and the various drivers. The shape of the points represents the attribution-evidence categories defined in Table 2. The trend likelihood comparison categories defined as “Stable” refers to the “Unlikely” or “Uncertain” trend likelihood categories defined in row one of Table 2. Each quadrant includes the total percentage of sites that are defined as having “Robust” or “Moderate” evidence, and the top middle percentage is the total percentage of sites that are defined as “Limited” or “Unknown” evidence. Percentages may not total 100 due to rounding.



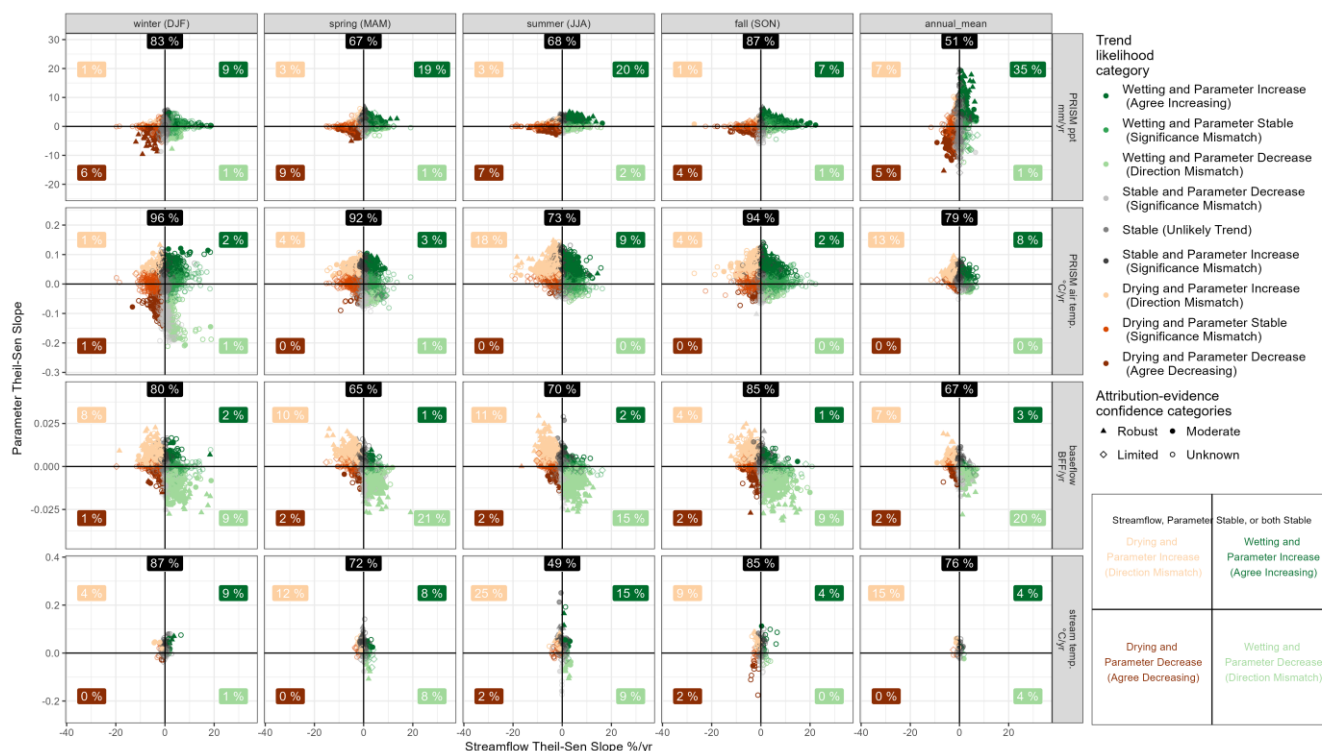
790 **Fig. A5: Seasonal stream temperature trends for 2000-2020 and attribution evidence results by climate, baseflow, and streamflow**
drivers. Winter = December, January, and February (DJF), Spring = March, April, and May (MAM), Summer = June, July, and
795 August (JJA), and Fall = September, October and November (SON). The location of the points represents the monthly or annual
Theil-Sen slope values for stream temperature in degrees Celsius per year plotted against potential attribution parameters of PRISM
precipitation (PRISM ppt) in millimetres per year, PRISM average air temperature (PRISM air temp) in degrees Celsius per year,
baseflow fraction (BFF) per year, and streamflow in percent change per year. For example, one site may have as many as three
monthly data points represented in one seasonal facet. The colour of the points represents the comparison trend likelihood categories
for stream temperature and the various drivers. The shape of the points represents the attribution-evidence categories defined in
Table 2. The trend likelihood comparison categories defined as “Stable” refers to the “Unlikely” or “Uncertain” trend likelihood
800 categories defined in row one of Table 2. Each quadrant includes the total percentage of sites that are defined as having “Robust”
or “Moderate” evidence, and the top middle percentage is the total percentage of sites that are defined as “Limited” or “Unknown”
evidence. Percentages may not total 100 due to rounding.



805 **Fig. A6: Seasonal streamflow trends for 1980-2020 and attribution evidence results by climate, baseflow, and streamflow drivers.**
 Winter = December, January, and February (DJF), Spring = March, April, and May (MAM), Summer = June, July, and August (JJA), and Fall = September, October and November (SON). The location of the points represents the monthly or annual Theil-Sen slope values for stream temperature in degrees Celsius per year plotted against parameters of PRISM precipitation (PRISM ppt) in millimetres per year, PRISM average air temperature (PRISM air temp) in degrees Celsius per year, baseflow fraction (BFF) per year, and stream temperature in degrees Celsius per year. For example, one site may have as many as three monthly data points represented in one seasonal facet. The colour of the points represents the comparison trend likelihood categories for stream temperature and the various drivers. The shape of the points represents the attribution-evidence categories defined in Table 2. The trend likelihood comparison categories defined as “Stable” refers to the “Unlikely” or “Uncertain” trend likelihood categories defined in row one of Table 2. Each quadrant includes the total percentage of sites that are defined as having “Robust” or “Moderate” evidence, and the top middle percentage is the total percentage of sites that are defined as “Limited” or “Unknown” evidence. Percentages may not total 100 due to rounding.

810

815



820 **Fig. A7: Seasonal streamflow trends for 1990-2020 and attribution evidence results by climate, baseflow, and streamflow drivers. Winter = December, January, and February (DJF), Spring = March, April, and May (MAM), Summer = June, July, and August (JJA), and Fall = September, October and November (SON). The location of the points represents the monthly or annual Theil-Sen slope values for stream temperature in degrees Celsius per year plotted against potential attribution parameters of PRISM precipitation (PRISM ppt) in millimetres per year, PRISM average air temperature (PRISM air temp) in degrees Celsius per year, baseflow fraction (BFF) per year, and stream temperature in degrees Celsius per year. For example, one site may have as many as three monthly data points represented in one seasonal facet. The colour of the points represents the comparison trend likelihood categories for stream temperature and the various drivers. The shape of the points represents the attribution-evidence categories defined in Table 2. The trend likelihood comparison categories defined as “Stable” refers to the “Unlikely” or “Uncertain” trend likelihood categories defined in row one of Table 2. Each quadrant includes the total percentage of sites that are defined as having “Robust” or “Moderate” evidence, and the top middle percentage is the total percentage of sites that are defined as “Limited” or “Unknown” evidence. Percentages may not total 100 due to rounding.**

825

830

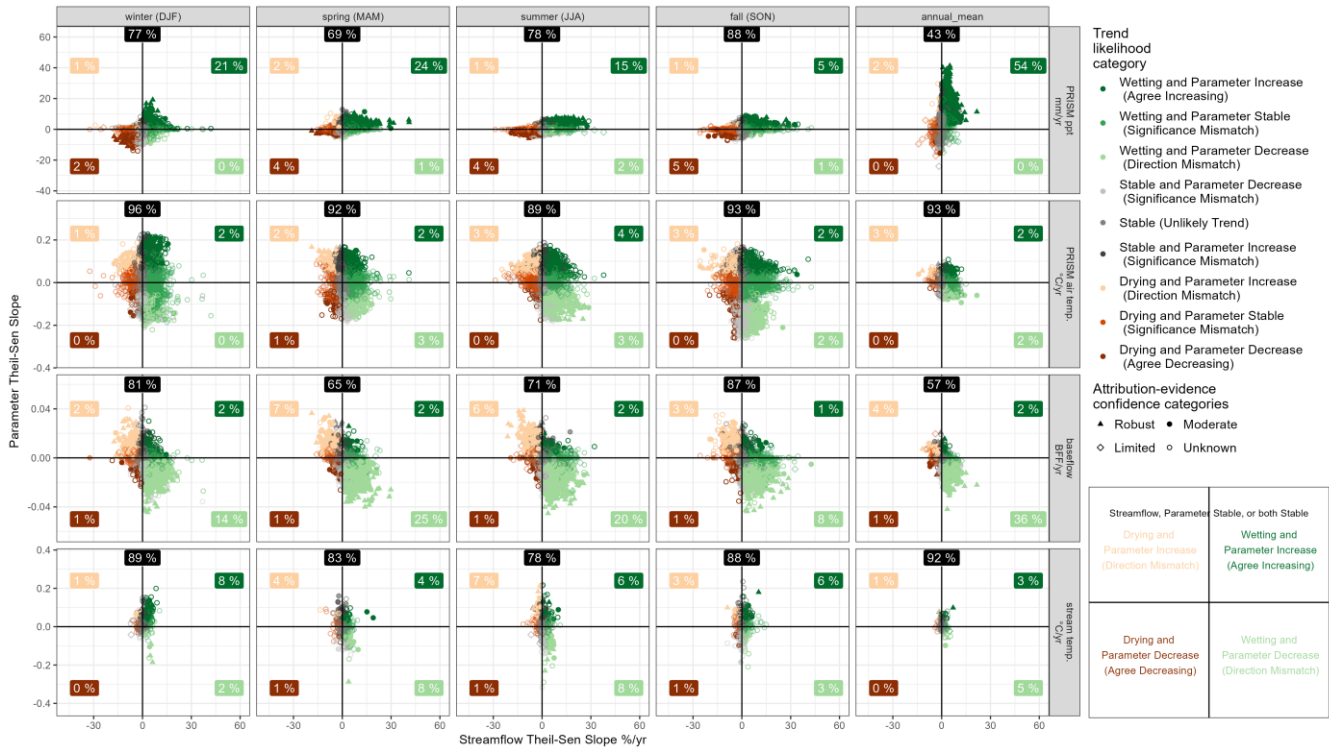
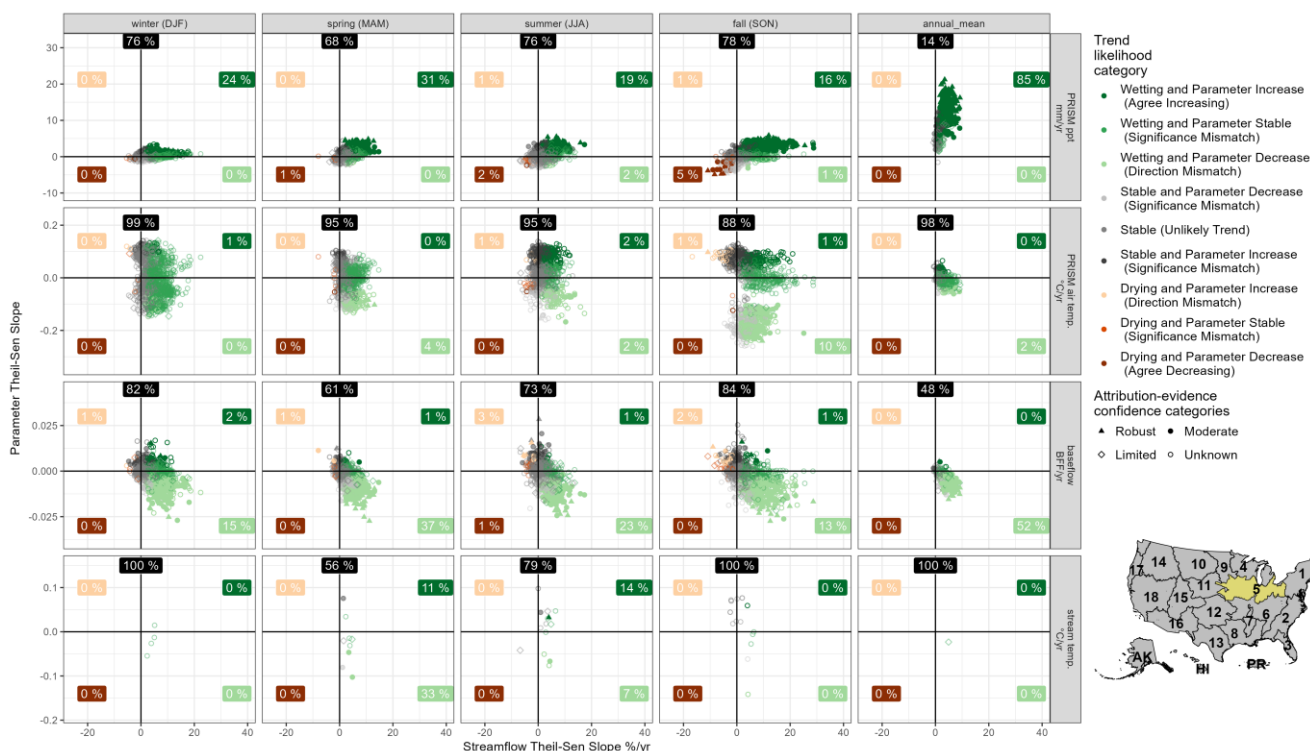


Fig. A8: Seasonal streamflow trends for 2000-2020 and attribution evidence results by climate, baseflow, and streamflow drivers. Winter = December, January, and February (DJF), Spring = March, April, and May (MAM), Summer = June, July, and August (JJA), and Fall = September, October and November (SON). The location of the points represents the monthly or annual Theil-Sen slope values for stream temperature in degrees Celsius per year plotted against potential attribution parameters of PRISM precipitation (PRISM ppt) in millimetres per year, PRISM average air temperature (PRISM air temp) in degrees Celsius per year, baseflow fraction (BFF) per year, and stream temperature in degrees Celsius per year. For example, one site may have as many as three monthly data points represented in one seasonal facet. The colour of the points represents the comparison trend likelihood categories for stream temperature and the various drivers. The shape of the points represents the attribution-evidence categories defined in Table 2. The trend likelihood comparison categories defined as “Stable” refers to the “Unlikely” or “Uncertain” trend likelihood categories defined in row one of Table 2. Each quadrant includes the total percentage of sites that are defined as having “Robust” or “Moderate” evidence, and the top middle percentage is the total percentage of sites that are defined as “Limited” or “Unknown” evidence. Percentages may not total 100 due to rounding.

835

840

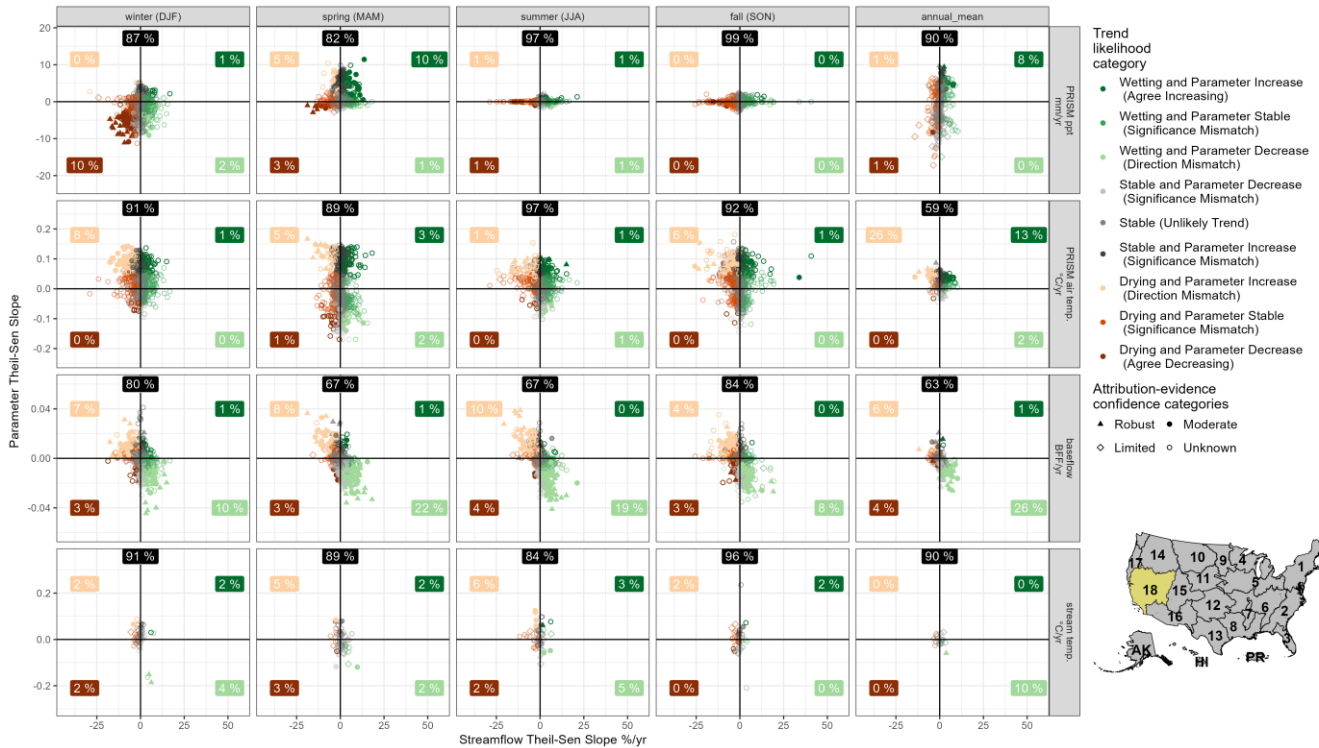


845

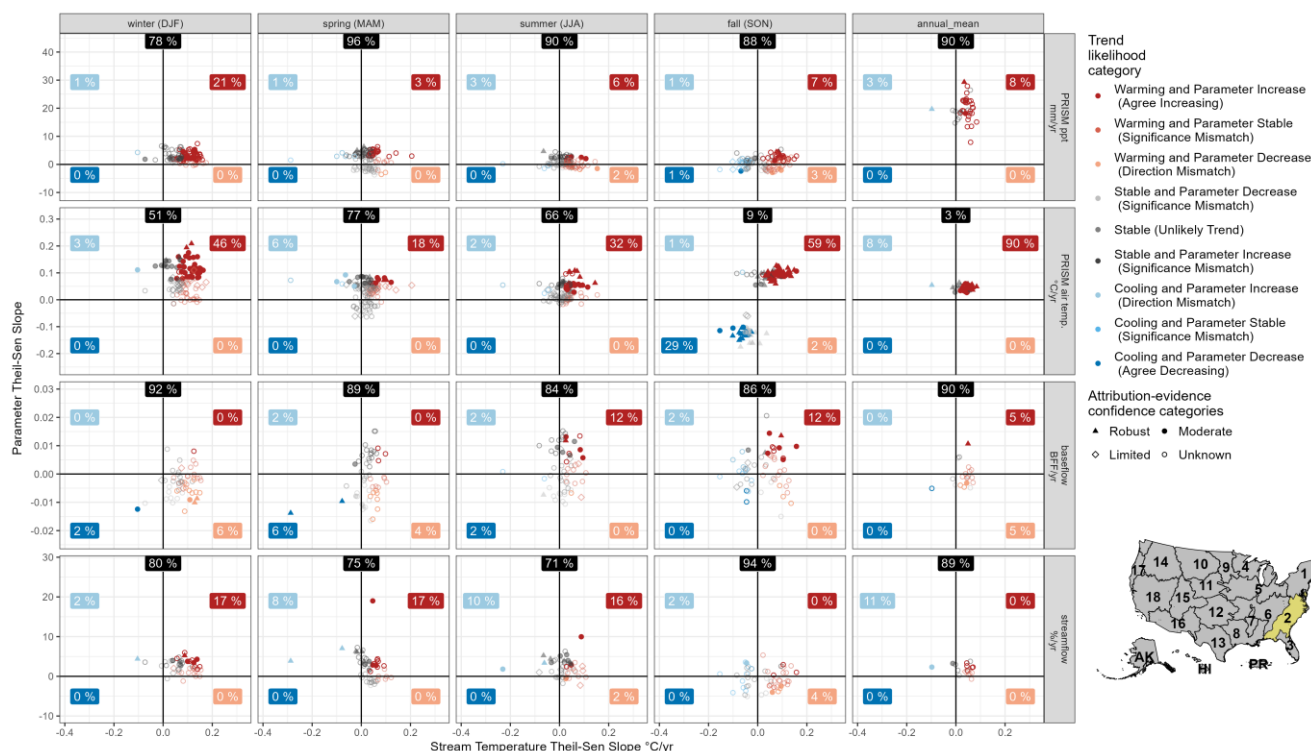
850

855

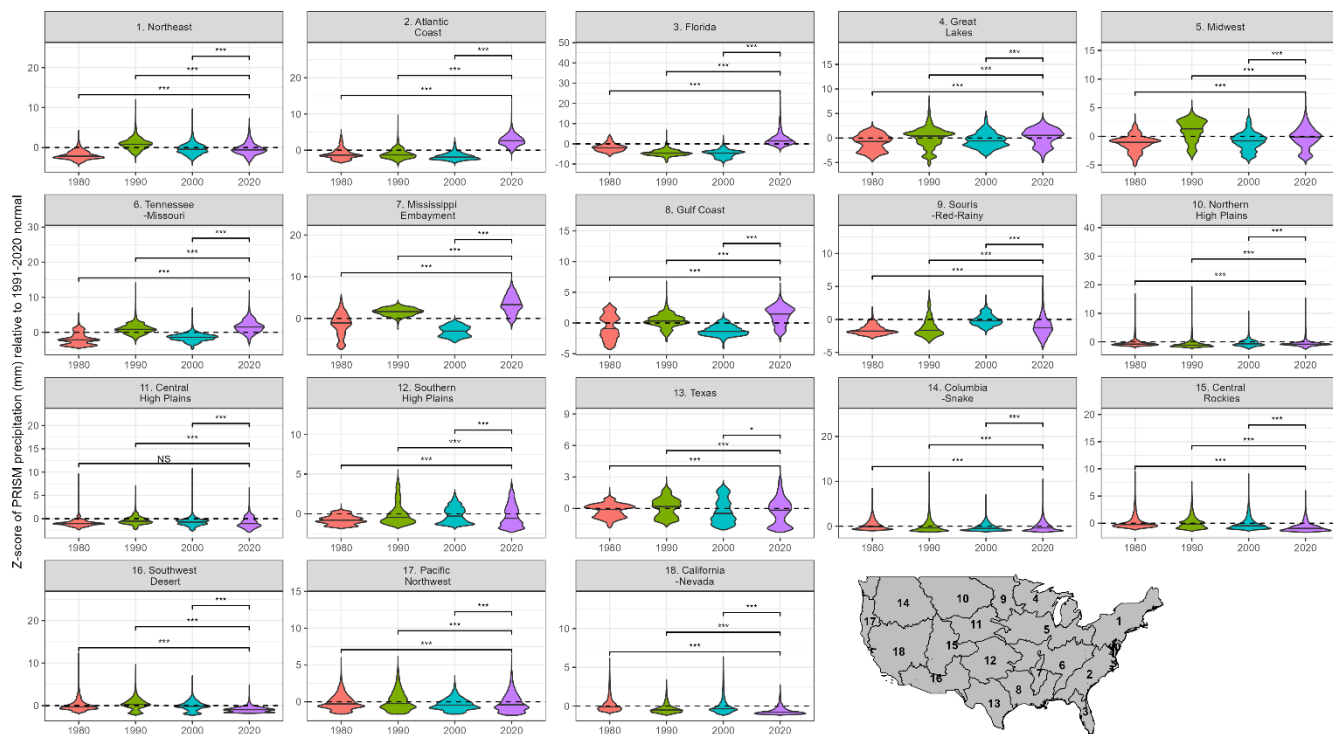
Fig. A9: The Midwest hydrologic region seasonal streamflow trends for 2000-2020 and attribution evidence results by climate, baseflow, and streamflow drivers. Winter = December, January, and February (DJF), Spring = March, April, and May (MAM), Summer = June, July, and August (JJA), and Fall = September, October and November (SON). The location of the points represents the monthly or annual Theil-Sen slope values for stream temperature in degrees Celsius per year plotted against potential attribution parameters of PRISM precipitation (PRISM ppt) in millimetres per year, PRISM average air temperature (PRISM air temp) in degrees Celsius per year, baseflow fraction (BFF) per year, and stream temperature in degrees Celsius per year. For example, one site may have as many as three monthly data points represented in one seasonal facet. The colour of the points represents the comparison trend likelihood categories for stream temperature and the various drivers. The shape of the points represents the attribution-evidence categories defined in Table 2. The trend likelihood comparison categories defined as “Stable” refers to the “Unlikely” or “Uncertain” trend likelihood categories defined in row one of Table 2. Each quadrant includes the total percentage of sites that are defined as having “Robust” or “Moderate” evidence, and the top middle percentage is the total percentage of sites that are defined as “Limited” or “Unknown” evidence. Percentages may not total 100 due to rounding.



860 **Fig. A10: The California-Nevada hydrologic region seasonal streamflow trends for 2000-2020 and attribution evidence results by**
865 climate, baseflow, and streamflow drivers. Winter = December, January, and February (DJF), Spring = March, April, and May
(MAM), Summer = June, July, and August (JJA), and Fall = September, October and November (SON). The location of the points
represents the monthly or annual Theil-Sen slope values for stream temperature in degrees Celsius per year plotted against potential
attribution parameters of PRISM precipitation (PRISM ppt) in millimetres per year, PRISM average air temperature (PRISM air
temp) in degrees Celsius per year, baseflow fraction (BFF) per year, and stream temperature in degrees Celsius per year. For
870 example, one site may have as many as three monthly data points represented in one seasonal facet. The colour of the points
represents the comparison trend likelihood categories for stream temperature and the various drivers. The shape of the points
represents the attribution-evidence confidence categories defined in Table 2. The trend likelihood comparison categories defined as “Stable”
refers to the “Unlikely” or “Uncertain” trend likelihood categories defined in row one of Table 2. Each quadrant includes the total
percentage of sites that are defined as having “Robust” or “Moderate” evidence, and the top middle percentage is the total
percentage of sites that are defined as “Limited” or “Unknown” evidence. Percentages may not total 100 due to rounding.

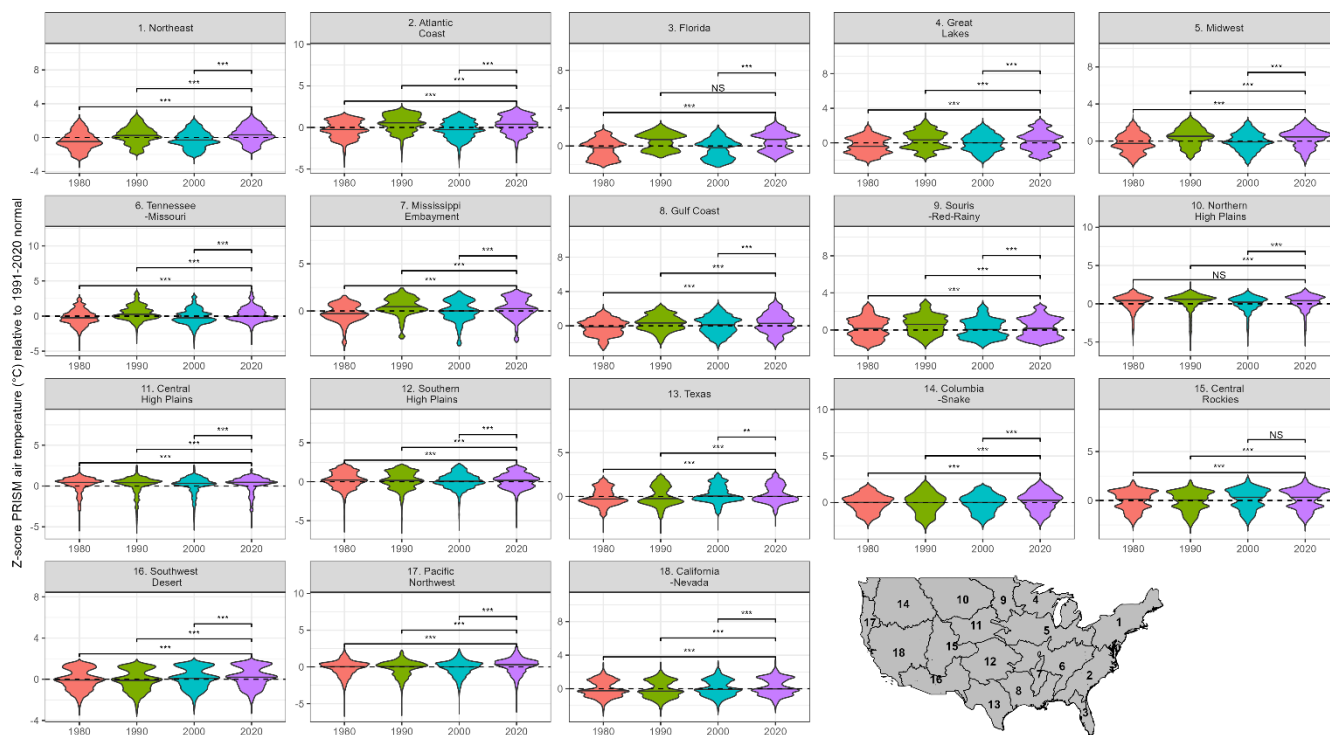


875 **Fig. A11: The Atlantic Coast hydrologic region seasonal stream temperature trends for 2000–2020 and attribution evidence results by climate, baseflow, and streamflow drivers. Winter = December, January, and February (DJF), Spring = March, April, and May**
880 (MAM), Summer = June, July, and August (JJA), and Fall = September, October and November (SON). The location of the points represents the monthly or annual Theil-Sen slope values for stream temperature in degrees Celsius per year plotted against potential attribution parameters of PRISM precipitation (PRISM ppt) in millimetres per year, PRISM average air temperature (PRISM air temp) in degrees Celsius per year, baseflow fraction (BFF) per year, and streamflow in percent change per year. For example, one site may have as many as three monthly data points represented in one seasonal facet. The colour of the points represents the comparison trend likelihood categories for stream temperature and the various drivers. The shape of the points represents the attribution-evidence categories defined in Table 2. The trend likelihood comparison categories defined as “Stable” refers to the “Unlikely” or “Uncertain” trend likelihood categories defined in row one of Table 2. Each quadrant includes the total percentage of sites that are defined as having “Robust” or “Moderate” evidence, and the top middle percentage is the total percentage of sites that are defined as “Limited” or “Unknown” evidence. Percentages may not total 100 due to rounding.



885

Fig. A12: The PRISM precipitation z-score trend period starting years (1980, 1990, and 2000) and ending year (2020) comparison with 1991-2020 precipitation normal by hydrologic regions. The non-parametric Wilcoxon test was performed between each starting year and 2020, where, * = p-value < 0.001, ** = p-value < 0.01, * = p-value < 0.05, NS = p-value > 0.05.**



890 **Fig. A13: The PRISM average air temperature z-score trend period starting years (1980, 1990, and 2000) and ending year (2020) comparison with 1991-2020 air temperature normal by hydrologic regions. The non-parametric Wilcoxon test was performed between each starting year and 2020, where, *** = p-value < 0.001, ** = p-value < 0.01, * = p-value < 0.05, NS = p-value > 0.05.s**



895 **Figure A14: Map of CONUS, Alaska, Hawaii, and Puerto Rico with the hydrologic regions overlaid. The regions are defined as: 1 = Northeast, 2 = Atlantic Coast, 3 = Florida, 4 = Great Lakes, 5 = Midwest, 6 = Tennessee-Missouri, 7 = Mississippi Embayment, 8 = Gulf Coast, 9 = Souris-Red-Rainy, 10 = Northern High Plains, 11 = Central High Plains, 12 = Southern High Plains, 13 = Texas, 14 = Columbia-Snake, 15 = Central Rockies, 16 = Southwest Desert, 17 = Pacific Northwest, 18 = California-Nevada, AK = Alaska, HI = Hawaii, PR = Puerto Rico (Van Metre et al., 2020)**

900 **Code availability**

Stagnitta T.J., Ebel, B.A., Johnson Z.C., and Martinez A.J., 2026, Decadal Trends in Streamflow and Stream Temperature across the Contiguous United States, Alaska, Hawaii, and Puerto Rico (1980–2020): Input Data and R Code: U.S. Geological Survey data release, <https://doi.org/10.5066/P1TWJWMO>.

Data availability

905 Stagnitta T.J., Ebel, B.A., Johnson Z.C., and Martinez A.J., 2026, Decadal Trends in Streamflow and Stream Temperature across the Contiguous United States, Alaska, Hawaii, and Puerto Rico (1980–2020): Input Data and R Code: U.S. Geological Survey data release, <https://doi.org/10.5066/P1TWJWMO>.



Author contribution

TS led the project; TS, ZJ, BE, and JA analysed the data; TS created all figures; TS, ZJ, BE, and JA wrote the draft manuscript;
910 TS, ZJ, and BE revised the draft manuscript.

Competing interests

The authors declare that they have no conflict of interest.

Disclaimer

Any use of trade, firm, or product names is for descriptive purposes only and does not imply endorsement by the U.S.
915 government.

Acknowledgements

We would like to thank Robin Glas and Caelan Simeone of the U.S. Geological Survey for their detailed reviews of this manuscript and Sydney Foks for her review of the companion U.S. Geological Survey data release. In addition, we thank Gretchen Oelsner for her leadership and guidance with developing this study.

920 Financial support

This work was completed as a part of the U.S. Geological Survey Integrated Water Availability Assessments Program. Funding for this effort comes from the U.S. Geological Survey National Water Quality Program and the Water Availability and Use Science Program.

References

- 925 Aguado, E., Cayan, D., Riddle, L., and Roos, M.: Climatic Fluctuations and the Timing of West Coast Streamflow, *J. Climate*, 5, 1468–1483, [https://doi.org/10.1175/1520-0442\(1992\)005%253C1468:CFATTO%253E2.0.CO;2](https://doi.org/10.1175/1520-0442(1992)005%253C1468:CFATTO%253E2.0.CO;2), 1992.
- Anandhi, A., Crandall, C., and Bentley, C.: Hydrologic Characteristics of Streamflow in the Southeast Atlantic and Gulf Coast Hydrologic Region during 1939–2016 and Conceptual Map of Potential Impacts, *Hydrology*, 5, 42, <https://doi.org/10.3390/hydrology5030042>, 2018.
- 930 Anderson, J. R., Hardy, E. E., Roach, J. T., and Witmer, R. E.: A land use and land cover classification system for use with remote sensor data, 1976.



- Arismendi, I., Safeeq, M., Johnson, S. L., Dunham, J. B., and Haggerty, R.: Increasing synchrony of high temperature and low flow in western North American streams: double trouble for coldwater biota?, *Hydrobiologia*, 712, 61–70, <https://doi.org/10.1007/s10750-012-1327-2>, 2013.
- 935 Ayers, J. R., Villarini, G., Jones, C., and Schilling, K.: Changes in monthly baseflow across the U.S. Midwest, *Hydrological Processes*, 33, 748–758, <https://doi.org/10.1002/hyp.13359>, 2019.
- Ayers, J. R., Villarini, G., Schilling, K., and Jones, C.: Projected changes in monthly baseflow across the U.S. Midwest, *Intl Journal of Climatology*, 41, 5536–5549, <https://doi.org/10.1002/joc.7140>, 2021.
- Ayers, J. R., Villarini, G., Schilling, K., Jones, C., Brookfield, A., Zipper, S. C., and Farmer, W. H.: The Role of Climate in
940 Monthly Baseflow Changes across the Continental United States, *J. Hydrol. Eng.*, 27, 04022006, [https://doi.org/10.1061/\(ASCE\)HE.1943-5584.0002170](https://doi.org/10.1061/(ASCE)HE.1943-5584.0002170), 2022.
- Barnett, T. P., Pierce, D. W., Hidalgo, H. G., Bonfils, C., Santer, B. D., Das, T., Bala, G., Wood, A. W., Nozawa, T., Mirin, A. A., Cayan, D. R., and Dettinger, M. D.: Human-Induced Changes in the Hydrology of the Western United States, *Science*, 319, 1080–1083, <https://doi.org/10.1126/science.1152538>, 2008.
- 945 Bassiouni, M. and Oki, D. S.: Trends and shifts in streamflow in Hawai‘i, 1913–2008, *Hydrological Processes*, 27, 1484–1500, <https://doi.org/10.1002/hyp.9298>, 2013.
- Beighley, R. E., Melack, J. M., and Dunne, T.: Impacts of California’s climatic regimes and coastal land use change on streamflow characteristics, *J American Water Resour Assoc*, 39, 1419–1433, <https://doi.org/10.1111/j.1752-1688.2003.tb04428.x>, 2003.
- 950 Berg, N. and Hall, A.: Increased Interannual Precipitation Extremes over California under Climate Change, *Journal of Climate*, 28, 6324–34, 2015.
- Blodgett, D. L. and Johnson, J. M.: nhdplusTools: Tools for Accessing and Working with the NHDPlus, <https://doi.org/10.5066/P97AS8JD>, 2022.
- Botero-Acosta, A., Ficklin, D. L., Ehsani, N., and Knouft, J. H.: Climate induced changes in streamflow and water temperature
955 in basins across the Atlantic Coast of the United States: An opportunity for nature-based regional management, *Journal of Hydrology: Regional Studies*, 44, 101202, <https://doi.org/10.1016/j.ejrh.2022.101202>, 2022.
- Brogan, C., Burgholzer, R., Keys, T., Kleiner, J., Shortridge, J., and Scott, D.: The Cumulative Role of Impoundments in Streamflow Alteration, *J American Water Resour Assoc*, 58, 119–133, <https://doi.org/10.1111/1752-1688.12979>, 2022.
- Brown, T. C., Mahat, V., and Ramirez, J. A.: Adaptation to Future Water Shortages in the United States Caused by Population
960 Growth and Climate Change, *Earth’s Future*, 7, 219–234, <https://doi.org/10.1029/2018EF001091>, 2019.
- Brun, J. and Barros, A. P.: Mapping the role of tropical cyclones on the hydroclimate of the southeast United States: 2002–2011, *Intl Journal of Climatology*, 34, 494–517, <https://doi.org/10.1002/joc.3703>, 2014.
- Carlisle, D. M., Wolock, D. M., Howard, J. K., Grantham, T. E., Fesenmyer, K., and Wieczorek, M.: Estimating natural monthly streamflows in California and the likelihood of anthropogenic modification:, U.S. Geological Survey, Reston, VA,
965 <https://doi.org/10.3133/ofr20161189>, 2016.



- Cayan, D. R., Tyree, M., Kunkel, K. E., Castro, C., Gershunov, A., Barsugli, J., Ray, A. J., Overpeck, J., Anderson, M., Russell, J., Rajagopalan, B., Rangwala, I., Duffy, P., and Barlow, M.: Future Climate: Projected Average, in: Assessment of Climate Change in the Southwest United States, edited by: Garfin, G., Jardine, A., Merideth, R., Black, M., and LeRoy, S., Island Press/Center for Resource Economics, Washington, DC, 101–125, https://doi.org/10.5822/978-1-61091-484-0_6, 2013.
- 970 Chalise, D. R., Aiyyer, A., and Sankarasubramanian, A.: Tropical Cyclones' Contribution to Seasonal Precipitation and Streamflow Over the Southeastern and Southcentral United States, *Geophysical Research Letters*, 48, e2021GL094738, <https://doi.org/10.1029/2021GL094738>, 2021.
- Chegini, T., Li, H.-Y., and Leung, L.: HyRiver: Hydroclimate Data Retriever, *JOSS*, 6, 3175, <https://doi.org/10.21105/joss.03175>, 2021.
- 975 Clilverd, H. M., Tsang, Y., Infante, D. M., Lynch, A. J., and Strauch, A. M.: Long-term streamflow trends in Hawai'i and implications for native stream fauna, *Hydrological Processes*, 33, 699–719, <https://doi.org/10.1002/hyp.13356>, 2019.
- Constantz, J.: Interaction between stream temperature, streamflow, and groundwater exchanges in alpine streams, *Water Resources Research*, 34, 1609–1615, <https://doi.org/10.1029/98WR00998>, 1998.
- Curran, J. H. and Biles, F. E.: Identification of Seasonal Streamflow Regimes and Streamflow Drivers for Daily and Peak
- 980 Flows in Alaska, *Water Resources Research*, 57, e2020WR028425, <https://doi.org/10.1029/2020WR028425>, 2021.
- Davies, P. M., Naiman, R. J., Warfe, D. M., Pettit, N. E., Arthington, A. H., and Bunn, S. E.: Flow–ecology relationships: closing the loop on effective environmental flows, *Mar. Freshwater Res.*, 65, 133, <https://doi.org/10.1071/mf13110>, 2014.
- DeGaetano, A. T.: Time-Dependent Changes in Extreme-Precipitation Return-Period Amounts in the Continental United States, *Journal of Applied Meteorology and Climatology*, 48, 2086–2099, <https://doi.org/10.1175/2009jamec2179.1>, 2009.
- 985 Diffenbaugh, N. S., Swain, D. L., and Touma, D.: Anthropogenic warming has increased drought risk in California, *Proc. Natl. Acad. Sci. U.S.A.*, 112, 3931–3936, <https://doi.org/10.1073/pnas.1422385112>, 2015.
- Dralle, D. N., Karst, N. J., and Thompson, S. E.: Dry season streamflow persistence in seasonal climates, *Water Resources Research*, 52, 90–107, <https://doi.org/10.1002/2015WR017752>, 2016.
- Dudley, R. W., Hodgkins, G. A., McHale, M. R., Kolian, M. J., and Renard, B.: Trends in snowmelt-related streamflow timing
- 990 in the conterminous United States, *Journal of Hydrology*, 547, 208–221, <https://doi.org/10.1016/j.jhydrol.2017.01.051>, 2017.
- Dudley, R. W., Hirsch, R. M., Archfield, S. A., Blum, A. G., and Renard, B.: Low streamflow trends at human-impacted and reference basins in the United States, *Journal of Hydrology*, 580, 124254, <https://doi.org/10.1016/j.jhydrol.2019.124254>, 2020.
- Engström, J. and Waylen, P.: The changing hydroclimatology of Southeastern U.S., *Journal of Hydrology*, 548, 16–23, <https://doi.org/10.1016/j.jhydrol.2017.02.039>, 2017.
- 995 Ficklin, D. L., Robeson, S. M., and Knouft, J. H.: Impacts of recent climate change on trends in baseflow and stormflow in United States watersheds, *Geophysical Research Letters*, 43, 5079–5088, <https://doi.org/10.1002/2016GL069121>, 2016.
- Ford, C. M., Kendall, A. D., and Hyndman, D. W.: Snowpacks decrease and streamflows shift across the eastern US as winters warm, *Science of The Total Environment*, 793, 148483, <https://doi.org/10.1016/j.scitotenv.2021.148483>, 2021.



- Foufoula-Georgiou, E., Takbiri, Z., Czuba, J. A., and Schwenk, J.: The change of nature and the nature of change in agricultural landscapes: Hydrologic regime shifts modulate ecological transitions, *Water Resources Research*, 51, 6649–6671, <https://doi.org/10.1002/2015WR017637>, 2015.
- Frans, C., Istanbuluoglu, E., Mishra, V., Munoz-Arriola, F., and Lettenmaier, D. P.: Are climatic or land cover changes the dominant cause of runoff trends in the Upper Mississippi River Basin?, *Geophysical Research Letters*, 40, 1104–1110, <https://doi.org/10.1002/grl.50262>, 2013.
- 1005 Grantham, T. E. W., Carlisle, D. M., McCabe, G. J., and Howard, J. K.: Sensitivity of streamflow to climate change in California, *Climatic Change*, 149, 427–441, <https://doi.org/10.1007/s10584-018-2244-9>, 2018.
- Gupta, A., Carroll, R. W. H., and McKenna, S. A.: Changes in streamflow statistical structure across the United States due to recent climate change, *Journal of Hydrology*, 620, 129474, <https://doi.org/10.1016/j.jhydrol.2023.129474>, 2023.
- Gupta, S. C., Baeumler, N. W., Kessler, A. C., Brown, M. K., Schuh, W. M., and Wolf, K. A.: Increased Precipitation as the Main Driver of Increased Streamflow in Tile-Drained Watersheds of the Upper Midwestern U.S., *Transactions of the ASABE*, 61, 207–222, <https://doi.org/10.13031/trans.12279>, 2018.
- 1010 Hart, E. and Bell, K.: prism: Access data from the Oregon State Prism climate project, <https://doi.org/10.5281/ZENODO.33663>, 2015.
- Hayhoe, K., Wake, C. P., Huntington, T. G., Luo, L., Schwartz, M. D., Sheffield, J., Wood, E., Anderson, B., Bradbury, J., DeGaetano, A., Troy, T. J., and Wolfe, D.: Past and future changes in climate and hydrological indicators in the US Northeast, *Clim Dyn*, 28, 381–407, <https://doi.org/10.1007/s00382-006-0187-8>, 2007.
- He, M., Russo, M., and Anderson, M.: Predictability of Seasonal Streamflow in a Changing Climate in the Sierra Nevada, *Climate*, 4, 57, <https://doi.org/10.3390/cli4040057>, 2016.
- Headman, A. O. and Hecht, J. S.: Identifying post-reservoir construction periods for monotonic trend analysis at streamgages in the United States (ver. 2.1, May 2025), <https://doi.org/10.5066/P922P61Z>, 2025.
- 1020 Hecht, J. S., Johnson, Z. C., and Dunne, K. A.: Long-term monotonic trends in annual and monthly streamflow metrics at streamgages in the United States (ver. 2.0, October 2024), <https://doi.org/10.5066/P9VBR38I>, 2024.
- Helsel, D. R., Hirsch, R. M., Ryberg, K. R., Archfield, S. A., and Gilroy, E. J.: *Statistical methods in water resources*, 2020.
- Hidalgo, H. G., Das, T., Dettinger, M. D., Cayan, D. R., Pierce, D. W., Barnett, T. P., Bala, G., Mirin, A., Wood, A. W., Bonfils, C., Santer, B. D., and Nozawa, T.: Detection and Attribution of Streamflow Timing Changes to Climate Change in the Western United States, *Journal of Climate*, 22, 3838–3855, <https://doi.org/10.1175/2009JCLI2470.1>, 2009.
- 1025 Hijmans, R.: terra:: Spatial Data Analysis, 2025.
- Hirsch, R. M., Archfield, S. A., and De Cicco, L. A.: A bootstrap method for estimating uncertainty of water quality trends, *Environmental Modelling & Software*, 73, 148–166, <https://doi.org/10.1016/j.envsoft.2015.07.017>, 2015.
- 1030 Hollander, M., A. Wolfe, D., and Chicken, E.: *Nonparametric Statistical Methods*, 1st ed., Wiley, <https://doi.org/10.1002/9781119196037>, 2015.



- Horne, J. P. and Hubbart, J. A.: A Spatially Distributed Investigation of Stream Water Temperature in a Contemporary Mixed-Land-Use Watershed, *Water*, 12, 1756, <https://doi.org/10.3390/w12061756>, 2020.
- Hou, Y., Han, J., Woods, R., Guo, Y., and Yang, Y.: Understanding Long-Term Streamflow Response to Snowfall Change: Insights From a Multivariate Analysis, *Water Resources Research*, 61, e2024WR038215, <https://doi.org/10.1029/2024WR038215>, 2025.
- Huh, S., Dickey, D. A., Meador, M. R., and Ruhl, K. E.: Temporal analysis of the frequency and duration of low and high streamflow: years of record needed to characterize streamflow variability, *Journal of Hydrology*, 310, 78–94, <https://doi.org/10.1016/j.jhydrol.2004.12.008>, 2005.
- 1040 Intergovernmental Panel On Climate Change (IPCC): Climate Change 2022 – Impacts, Adaptation and Vulnerability: Working Group II Contribution to the Sixth Assessment Report of the Intergovernmental Panel on Climate Change, 1st ed., Cambridge University Press, <https://doi.org/10.1017/9781009325844>, 2023.
- Isaak, D. J., Wollrab, S., Horan, D., and Chandler, G.: Climate change effects on stream and river temperatures across the northwest U.S. from 1980–2009 and implications for salmonid fishes, *Climatic Change*, 113, 499–524, <https://doi.org/10.1007/s10584-011-0326-z>, 2012.
- 1045 Isaak, D. J., Wenger, S. J., Peterson, E. E., Ver Hoef, J. M., Nagel, D. E., Luce, C. H., Hostetler, S. W., Dunham, J. B., Roper, B. B., Wollrab, S. P., Chandler, G. L., Horan, D. L., and Parkes-Payne, S.: The NorWeST Summer Stream Temperature Model and Scenarios for the Western U.S.: A Crowd-Sourced Database and New Geospatial Tools Foster a User Community and Predict Broad Climate Warming of Rivers and Streams, *Water Resources Research*, 53, 9181–9205, <https://doi.org/10.1002/2017WR020969>, 2017.
- 1050 Johnson, M. F., Albertson, L. K., Algar, A. C., Dugdale, S. J., Edwards, P., England, J., Gibbins, C., Kazama, S., Komori, D., MacColl, A. D. C., Scholl, E. A., Wilby, R. L., De Oliveira Roque, F., and Wood, P. J.: Rising water temperature in rivers: Ecological impacts and future resilience, *WIREs Water*, 11, e1724, <https://doi.org/10.1002/wat2.1724>, 2024.
- Johnson, Z. C.: Long-term monotonic trends in annual and monthly stream temperature metrics at multi-source monitoring locations in the United States, <https://doi.org/10.5066/P9V10XSF>, 2025.
- 1055 Kalra, A., Piechota, T. C., Davies, R., and Tootle, G. A.: Changes in U.S. Streamflow and Western U.S. Snowpack, *J. Hydrol. Eng.*, 13, 156–163, [https://doi.org/10.1061/\(ASCE\)1084-0699\(2008\)13:3\(156\)](https://doi.org/10.1061/(ASCE)1084-0699(2008)13:3(156)), 2008.
- Kaushal, S. S., Likens, G. E., Jaworski, N. A., Pace, M. L., Sides, A. M., Seekell, D., Belt, K. T., Secor, D. H., and Wingate, R. L.: Rising stream and river temperatures in the United States, *Frontiers in Ecol & Environ*, 8, 461–466, <https://doi.org/10.1890/090037>, 2010.
- 1060 Kelleher, C. A., Golden, H. E., and Archfield, S. A.: Monthly river temperature trends across the US confound annual changes, *Environ. Res. Lett.*, 16, 104006, <https://doi.org/10.1088/1748-9326/ac2289>, 2021.
- Kelly, S. A., Takbiri, Z., Belmont, P., and Foufoula-Georgiou, E.: Human amplified changes in precipitation–runoff patterns in large river basins of the Midwestern United States, *Hydrol. Earth Syst. Sci.*, 21, 5065–5088, <https://doi.org/10.5194/hess-21-5065-2017>, 2017.
- 1065



- Kendall, M. G.: Rank Correlation Methods, London: Charles Griffin and Co. Ltd., Pp. vii + 160, 1948.
- Knight, D. B. and Davis, R. E.: Climatology of Tropical Cyclone Rainfall in the Southeastern United States, *Physical Geography*, 28, 126–147, <https://doi.org/10.2747/0272-3646.28.2.126>, 2007.
- Kochendorfer, J. P. and Hubbart, J. A.: The Roles of Precipitation Increases and Rural Land-Use Changes in Streamflow Trends in the Upper Mississippi River Basin, *Earth Interactions*, 14, 1–12, <https://doi.org/10.1175/2010EI316.1>, 2010.
- 1070 Konrad, C. P.: Non-linear baseflow separation model with parameters and results (ver. 2.0, October 2022), <https://doi.org/10.5066/P9AIPHEP>, 2022.
- Koutsoyiannis, D. and Montanari, A.: Statistical analysis of hydroclimatic time series: Uncertainty and insights, *Water Resources Research*, 43, 2006WR005592, <https://doi.org/10.1029/2006WR005592>, 2007.
- 1075 Kunkel, K. E., Stevens, L. E., Sun, L., Janssen, E., Weubbles, D., Konrad, C. E., Fuhrmann, C. M., Keim, B. D., Kruk, M. C., Billot, A., Needham, H., Shafer, M., and Dobson, J. G.: Regional Climate Trends and Scenarios for the U.S. National Climate Assessment : Part 2. Climate of the Southeast U.S., https://repository.library.noaa.gov/view/noaa/56807/noaa_56807_DS1.pdf, 2013.
- LeBlanc, R. T., Brown, R. D., and FitzGibbon, J. E.: Modeling the Effects of Land Use Change on the Water Temperature in Unregulated Urban Streams, *Journal of Environmental Management*, 49, 445–469, <https://doi.org/10.1006/jema.1996.0106>, 1997.
- 1080 Lettenmaier, D. P., Wood, E. F., and Wallis, J. R.: Hydro-Climatological Trends in the Continental United States, 1948–88, *J. Climate*, 7, 586–607, [https://doi.org/10.1175/1520-0442\(1994\)007%253C0586:HCTITC%253E2.0.CO;2](https://doi.org/10.1175/1520-0442(1994)007%253C0586:HCTITC%253E2.0.CO;2), 1994.
- Li, D., Wrzesien, M. L., Durand, M., Adam, J., and Lettenmaier, D. P.: How much runoff originates as snow in the western United States, and how will that change in the future?, *Geophysical Research Letters*, 44, 6163–6172, <https://doi.org/10.1002/2017GL073551>, 2017.
- 1085 Lins, H. F. and Slack, J. R.: Streamflow trends in the United States, *Geophysical Research Letters*, 26, 227–230, <https://doi.org/10.1029/1998GL900291>, 1999.
- Lins, H. F. and Slack, J. R.: Seasonal and Regional Characteristics of U.S. Streamflow Trends in the United States from 1940 to 1999, *Physical Geography*, 26, 489–501, <https://doi.org/10.2747/0272-3646.26.6.489>, 2005.
- 1090 Luković, J., Chiang, J. C. H., Blagojević, D., and Sekulić, A.: A Later Onset of the Rainy Season in California, *Geophysical Research Letters*, 48, e2020GL090350, <https://doi.org/10.1029/2020GL090350>, 2021.
- Mallakpour, I., Sadegh, M., and AghaKouchak, A.: A new normal for streamflow in California in a warming climate: Wetter wet seasons and drier dry seasons, *Journal of Hydrology*, 567, 203–211, <https://doi.org/10.1016/j.jhydrol.2018.10.023>, 2018.
- 1095 Mann, H. B.: Nonparametric Tests Against Trend, *Econometrica*, 13, 245–259, 1945.
- Martin, J. T., Pederson, G. T., Woodhouse, C. A., Cook, E. R., McCabe, G. J., Anchukaitis, K. J., Wise, E. K., Erger, P. J., Dolan, L., McGuire, M., Gangopadhyay, S., Chase, K. J., Littell, J. S., Gray, S. T., St. George, S., Friedman, J. M., Sauchyn, D. J., St-Jacques, J.-M., and King, J.: Increased drought severity tracks warming in the United States’ largest river basin, *Proc. Natl. Acad. Sci. U.S.A.*, 117, 11328–11336, <https://doi.org/10.1073/pnas.1916208117>, 2020.



- 1100 Mastrandrea, M. D., Field, C. B., Stocker, T. F., Edenhofer, O., Ebi, K. L., Frame, D. J., Held, H., Kriegler, E., Mach, K. J., Matschoss, P. R., Plattner, G.-K., Yohe, G. W., and Zwiers, F. W.: Guidance Note for Lead Authors of the IPCC Fifth Assessment Report on Consistent Treatment of Uncertainties. Intergovernmental Panel on Climate Change (IPCC), 2010.
- Maurer, E. P., Stewart, I. T., Bonfils, C., Duffy, P. B., and Cayan, D.: Detection, attribution, and sensitivity of trends toward earlier streamflow in the Sierra Nevada, *J. Geophys. Res.*, 112, 2006JD008088, <https://doi.org/10.1029/2006JD008088>, 2007.
- 1105 Maxwell, J. T., Soulé, P. T., Ortegren, J. T., and Knapp, P. A.: Drought-Busting Tropical Cyclones in the Southeastern Atlantic United States: 1950–2008, *Annals of the Association of American Geographers*, 102, 259–275, <https://doi.org/10.1080/00045608.2011.596377>, 2012.
- Mayer, T. D.: Controls of summer stream temperature in the Pacific Northwest, *Journal of Hydrology*, 475, 323–335, <https://doi.org/10.1016/j.jhydrol.2012.10.012>, 2012.
- 1110 McCabe, G. J. and Wolock, D. M.: A step increase in streamflow in the conterminous United States, *Geophysical Research Letters*, 29, <https://doi.org/10.1029/2002GL015999>, 2002.
- McCabe, G. J., Wolock, D. M., Lombard, M., Dudley, R. W., Hammond, J. C., Hecht, J. S., Hodgkins, G. A., Olson, C., Sando, R., Simeone, C., and Wiczorek, M.: A hydrologic perspective of major U.S. droughts, *Intl Journal of Climatology*, 43, 1234–1250, <https://doi.org/10.1002/joc.7904>, 2023.
- 1115 Melillo, J. M., Richmond, T., and Yohe, G. W.: Highlights of climate change impacts in the United States: The Third National Climate Assessment. U.S. Global Change Research Program, U.S. Environmental Protection Agency, 148 pp., 2014.
- Misra, V., Michael, J.-P., Boyles, R., Chassignet, E. P., Griffin, M., and O’Brien, J. J.: Reconciling the Spatial Distribution of the Surface Temperature Trends in the Southeastern United States, *Journal of Climate*, 25, 3610–3618, <https://doi.org/10.1175/JCLI-D-11-00170.1>, 2012.
- 1120 Morales-Marín, L. A., Rokaya, P., Sanyal, P. R., Sereda, J., and Lindenschmidt, K. E.: Changes in streamflow and water temperature affect fish habitat in the Athabasca River basin in the context of climate change, *Ecological Modelling*, 407, 108718, <https://doi.org/10.1016/j.ecolmodel.2019.108718>, 2019.
- Mote, P. W., Parson, E. A., Hamlet, A. F., Keeton, W. S., Lettenmaier, D., Mantua, N., Miles, E. L., Peterson, D. W., Peterson, D. L., Slaughter, R., and Snover, A. K.: Preparing for Climatic Change: The Water, Salmon, and Forests of the Pacific Northwest, *Climatic Change*, 61, 45–88, <https://doi.org/10.1023/A:1026302914358>, 2003.
- 1125 Murphy, J. and Sprague, L.: Water-quality trends in US rivers: Exploring effects from streamflow trends and changes in watershed management, *Science of The Total Environment*, 656, 645–658, <https://doi.org/10.1016/j.scitotenv.2018.11.255>, 2019.
- Nelson, K. C. and Palmer, M. A.: Stream Temperature Surges Under Urbanization and Climate Change: Data, Models, and Responses¹, *J American Water Resour Assoc*, 43, 440–452, <https://doi.org/10.1111/j.1752-1688.2007.00034.x>, 2007.
- O’Driscoll, M., Clinton, S., Jefferson, A., Manda, A., and McMillan, S.: Urbanization Effects on Watershed Hydrology and In-Stream Processes in the Southern United States, *Water*, 2, 605–648, <https://doi.org/10.3390/w2030605>, 2010.



- Oliver, S. K., Appling, A. P., Watkins, D. D., Atshan, R. A., and Read, J. S.: Compilation of multi-agency water temperature observations for U.S. streams, 1894–2022, <https://doi.org/10.5066/P9EMWZ35>, 2024.
- 1135 Pan, Z., Arritt, R. W., Takle, E. S., Gutowski, W. J., Anderson, C. J., and Segal, M.: Altered hydrologic feedback in a warming climate introduces a “warming hole,” *Geophysical Research Letters*, 31, 2004GL020528, <https://doi.org/10.1029/2004GL020528>, 2004.
- Patterson, L. A., Lutz, B., and Doyle, M. W.: Streamflow Changes in the South Atlantic, United States During the Mid- and Late 20th Century, *J American Water Resour Assoc*, 48, 1126–1138, <https://doi.org/10.1111/j.1752-1688.2012.00674.x>, 2012.
- 1140 Portmann, R. W., Solomon, S., and Hegerl, G. C.: Spatial and seasonal patterns in climate change, temperatures, and precipitation across the United States, *Proc. Natl. Acad. Sci. U.S.A.*, 106, 7324–7329, <https://doi.org/10.1073/pnas.0808533106>, 2009.
- PRISM Group: PRISM, Oregon State University, [online] Available from: <https://prism.oregonstate.edu> [Accessed 11 February 2025], 2014.
- 1145 R Core Team: R: A Language and Environment for Statistical Computing, 2025.
- Read, E. K., Carr, L., De Cicco, L., Dugan, H. A., Hanson, P. C., Hart, J. A., Kreft, J., Read, J. S., and Winslow, L. A.: Water quality data for national-scale aquatic research: The Water Quality Portal, *Water Resources Research*, 53, 1735–1745, <https://doi.org/10.1002/2016WR019993>, 2017.
- Rice, J. S., Emanuel, R. E., Vose, J. M., and Nelson, S. A. C.: Continental U.S. streamflow trends from 1940 to 2009 and their relationships with watershed spatial characteristics, *Water Resources Research*, 51, 6262–6275, <https://doi.org/10.1002/2014WR016367>, 2015.
- 1150 Rice, J. S., Emanuel, R. E., and Vose, J. M.: The influence of watershed characteristics on spatial patterns of trends in annual scale streamflow variability in the continental U.S., *Journal of Hydrology*, 540, 850–860, <https://doi.org/10.1016/j.jhydrol.2016.07.006>, 2016.
- 1155 Rice, K. C. and Jastram, J. D.: Rising air and stream-water temperatures in Chesapeake Bay region, USA, *Climatic Change*, 128, 127–138, <https://doi.org/10.1007/s10584-014-1295-9>, 2015.
- Ryberg, K. R., ed.: Attribution of monotonic trends and change points in peak streamflow across the conterminous United States using a multiple working hypotheses framework, 1941–2015 and 1966–2015, 2022.
- Sagarika, S., Kalra, A., and Ahmad, S.: Evaluating the effect of persistence on long-term trends and analyzing step changes in streamflows of the continental United States, *Journal of Hydrology*, 517, 36–53, <https://doi.org/10.1016/j.jhydrol.2014.05.002>, 2014.
- 1160 Santiago, J. M., Muñoz-Mas, R., Solana-Gutiérrez, J., García De Jalón, D., Alonso, C., Martínez-Capel, F., Pórtoles, J., Monjo, R., and Ribalaygua, J.: Waning habitats due to climate change: the effects of changes in streamflow and temperature at the rear edge of the distribution of a cold-water fish, *Hydrol. Earth Syst. Sci.*, 21, 4073–4101, <https://doi.org/10.5194/hess-21-4073-2017>, 2017.
- 1165



- Schilling, K. E. and Libra, R. D.: Increased Baseflow in Iowa Over the Second Half of the 20TH CENTURY, *J American Water Resour Assoc*, 39, 851–860, <https://doi.org/10.1111/j.1752-1688.2003.tb04410.x>, 2003.
- Seager, R., Tzanova, A., and Nakamura, J.: Drought in the Southeastern United States: Causes, Variability over the Last Millennium, and the Potential for Future Hydroclimate Change*, *Journal of Climate*, 22, 5021–5045, <https://doi.org/10.1175/2009JCLI2683.1>, 2009.
- 1170 Segura, C., Caldwell, P., Sun, G., McNulty, S., and Zhang, Y.: A model to predict stream water temperature across the conterminous USA, *Hydrological Processes*, 29, 2178–2195, <https://doi.org/10.1002/hyp.10357>, 2015.
- Sen, P. K.: Estimates of the Regression Coefficient Based on Kendall’s Tau, *Journal of the American Statistical Association*, 63, 1379–1389, <https://doi.org/10.1080/01621459.1968.10480934>, 1968.
- 1175 Simeone, C., McCabe, G., Hecht, J., Hammond, J., Hodgkins, G., Olson, C., Wiczorek, M., and Wolock, D.: Low-flow period seasonality, trends, and climate linkages across the United States, *Hydrological Sciences Journal*, 69, 1387–1398, <https://doi.org/10.1080/02626667.2024.2369639>, 2024.
- Singh, N. K. and Basu, N. B.: The human factor in seasonal streamflows across natural and managed watersheds of North America, *Nat Sustain*, 5, 397–405, <https://doi.org/10.1038/s41893-022-00848-1>, 2022.
- 1180 Somers, K. A., Bernhardt, E. S., Grace, J. B., Hassett, B. A., Sudduth, E. B., Wang, S., and Urban, D. L.: Streams in the urban heat island: spatial and temporal variability in temperature, *Freshwater Science*, 32, 309–326, <https://doi.org/10.1899/12-046.1>, 2013.
- Stagnitta, T. J., Ebel, B. A., Johnson, Z. C., and Martinez, A. J.: Decadal Trends in Streamflow and Stream Temperature across the Contiguous United States, Alaska, Hawaii, and Puerto Rico (1980–2020): Input Data and R Code, <https://doi.org/10.5066/P1TWJWMQ>, 2026.
- 1185 Stets, E. G., Archer, A. A., Degnan, J. R., Erickson, M. L., Gorski, G., Medalie, L., and Scholl, M. A.: The National integrated water availability assessment, water years 2010–20, chap. A of U.S. Geological Survey Integrated Water Availability Assessment—2010–20, 2025.
- Stewart, I. T., Cayan, D. R., and Dettinger, M. D.: Changes toward Earlier Streamflow Timing across Western North America, *Journal of Climate*, 18, 1136–1155, <https://doi.org/10.1175/JCLI3321.1>, 2005.
- 1190 Sun, G., McNulty, S. G., Moore Myers, J. A., and Cohen, E. C.: Impacts of Multiple Stresses on Water Demand and Supply Across the Southeastern United States¹, *J American Water Resour Assoc*, 44, 1441–1457, <https://doi.org/10.1111/j.1752-1688.2008.00250.x>, 2008.
- Sun, N., Yearsley, J., Voisin, N., and Lettenmaier, D. P.: A spatially distributed model for the assessment of land use impacts on stream temperature in small urban watersheds, *Hydrol. Process.*, 29, 2331–2345, <https://doi.org/10.1002/hyp.10363>, 2015.
- 1195 Sun, N., Wigmosta, M. S., Judi, D., Yang, Z., Xiao, Z., and Wang, T.: Climatological analysis of tropical cyclone impacts on hydrological extremes in the Mid-Atlantic region of the United States, *Environ. Res. Lett.*, 16, 124009, <https://doi.org/10.1088/1748-9326/ac2d6a>, 2021.



- Swain, D. L.: A Shorter, Sharper Rainy Season Amplifies California Wildfire Risk, *Geophysical Research Letters*, 48, e2021GL092843, <https://doi.org/10.1029/2021GL092843>, 2021.
- Swain, D. L., Langenbrunner, B., Neelin, J. D., and Hall, A.: Increasing precipitation volatility in twenty-first-century California, *Nature Clim Change*, 8, 427–433, <https://doi.org/10.1038/s41558-018-0140-y>, 2018.
- Tamaddun, K., Kalra, A., and Ahmad, S.: Identification of Streamflow Changes across the Continental United States Using Variable Record Lengths, *Hydrology*, 3, 24, <https://doi.org/10.3390/hydrology3020024>, 2016.
- 1205 Tassone, S. J., Besterman, A. F., Buelo, C. D., Ha, D. T., Walter, J. A., and Pace, M. L.: Increasing heatwave frequency in streams and rivers of the United States, *Limnol Oceanogr Letters*, 8, 295–304, <https://doi.org/10.1002/lol2.10284>, 2023.
- Taylor, M. A., Clarke, L. A., Centella, A., Bezanilla, A., Stephenson, T. S., Jones, J. J., Campbell, J. D., Vichot, A., and Charlery, J.: Future Caribbean Climates in a World of Rising Temperatures: The 1.5 vs 2.0 Dilemma, *J. Climate*, 31, 2907–2926, <https://doi.org/10.1175/jcli-d-17-0074.1>, 2018.
- 1210 Theil, H.: A Rank-Invariant Method of Linear and Polynomial Regression Analysis, in: *Henri Theil's Contributions to Economics and Econometrics*, vol. 23, edited by: Raj, B. and Koerts, J., Springer Netherlands, Dordrecht, 345–381, https://doi.org/10.1007/978-94-011-2546-8_20, 1950.
- U.S. Geological Survey [USGS]: USGS Water Data for the Nation, [online] Available from: <https://doi.org/10.5066/F7P55KJN> (Accessed 18 November 2024), 2021.
- 1215 U.S. Geological Survey [USGS]: Annual National Land Cover Database (NLCD) Collection 1 Products, <https://doi.org/10.5066/P94UXNTS>, 2024.
- U.S. Geological Survey [USGS]: Hydro Network-Linked Data Index (NLDI), 2025.
- U.S. Geological Survey [USGS]: USGS National Hydrography Dataset Plus High Resolution National Release 1 FileGDB, [online] Available from: <https://doi.org/10.5066/P9WFOBQI> (Accessed 15 December 2025), 2022.
- 1220 Uzun, S., Tanir, T., Coelho, G. D. A., Souza De Lima, A. D., Cassalho, F., and Ferreira, C. M.: Changes in snowmelt runoff timing in the contiguous United States, *Hydrological Processes*, 35, e14430, <https://doi.org/10.1002/hyp.14430>, 2021.
- Van Metre, P. C., Qi, S., Deacon, J., Dieter, C., Driscoll, J. M., Fienen, M., Kenney, T., Lambert, P., Lesmes, D., Mason, C. A., Mueller-Solger, A., Musgrove, M., Painter, J., Rosenberry, D., Sprague, L., Tesoriero, A. J., Windham-Myers, L., and Wolock, D.: Prioritizing river basins for intensive monitoring and assessment by the US Geological Survey, *Environ Monit Assess*, 192, 458, <https://doi.org/10.1007/s10661-020-08403-1>, 2020.
- 1225 Van Vliet, M. T. H., Ludwig, F., Zwolsman, J. J. G., Weedon, G. P., and Kabat, P.: Global river temperatures and sensitivity to atmospheric warming and changes in river flow, *Water Resources Research*, 47, 2010WR009198, <https://doi.org/10.1029/2010WR009198>, 2011.
- Vose, R. S., Easterling, D. R., Kunkel, K. E., LeGrande, A. N., and Wehner, M. F.: Ch. 6: Temperature Changes in the United States. *Climate Science Special Report: Fourth National Climate Assessment, Volume I*, U.S. Global Change Research Program, <https://doi.org/10.7930/J0N29V45>, 2017.
- 1230



- Wang, Y., Zhang, X., Zhao, K., and Singh, D.: Streamflow in the United States: Characteristics, trends, regime shifts, and extremes, *Sci Data*, 11, 788, <https://doi.org/10.1038/s41597-024-03618-0>, 2024.
- Wang, Z. and Yang, Y.: Stationarity of High- and Low-Flows Under Climate Change and Human Interventions Across Global Catchments, *Earth and Space Science*, 11, e2023EA003456, <https://doi.org/10.1029/2023EA003456>, 2024.
- 1235 Webb, B. W., Clack, P. D., and Walling, D. E.: Water–air temperature relationships in a Devon river system and the role of flow, *Hydrological Processes*, 17, 3069–3084, <https://doi.org/10.1002/hyp.1280>, 2003.
- Wilbanks, K. A., Jackson, C. R., and Batzer, D. P.: Spatial Variability of Long-Term Streamflow Trends in the Southeastern United States, *River Research & Apps*, rra.4449, <https://doi.org/10.1002/rra.4449>, 2025.
- 1240 Wise, E. K., Woodhouse, C. A., McCabe, G. J., Pederson, G. T., and St-Jacques, J.-M.: Hydroclimatology of the Missouri River Basin, *Journal of Hydrometeorology*, 19, 161–182, <https://doi.org/10.1175/JHM-D-17-0155.1>, 2018.
- Woltemade, C. J. and Hawkins, T. W.: Stream Temperature Impacts Because of Changes in Air Temperature, Land Cover and Stream Discharge: Navarro River Watershed, California, USA: Stream Temperature Impacts, *River Res. Applic.*, 32, 2020–2031, <https://doi.org/10.1002/rra.3043>, 2016.
- 1245 Wu, H., Kimball, J. S., Elsner, M. M., Mantua, N., Adler, R. F., and Stanford, J.: Projected climate change impacts on the hydrology and temperature of Pacific Northwest rivers, *Water Resources Research*, 48, 2012WR012082, <https://doi.org/10.1029/2012WR012082>, 2012.
- Xiao, M., Udall, B., and Lettenmaier, D. P.: On the Causes of Declining Colorado River Streamflows, *Water Resources Research*, 54, 6739–6756, <https://doi.org/10.1029/2018wr023153>, 2018.
- 1250 Xu, X., Liu, W., Rafique, R., and Wang, K.: Revisiting Continental U.S. Hydrologic Change in the Latter Half of the 20th Century, *Water Resour Manage*, 27, 4337–4348, <https://doi.org/10.1007/s11269-013-0411-3>, 2013.
- Zahn, E., Welty, C., Smith, J. A., Kemp, S. J., Baeck, M., and Bou-Zeid, E.: The Hydrological Urban Heat Island: Determinants of Acute and Chronic Heat Stress in Urban Streams, *J American Water Resour Assoc*, 57, 941–955, <https://doi.org/10.1111/1752-1688.12963>, 2021.
- 1255 Zhang, Y.-K. and Schilling, K. E.: Increasing streamflow and baseflow in Mississippi River since the 1940s: Effect of land use change, *Journal of Hydrology*, 324, 412–422, <https://doi.org/10.1016/j.jhydrol.2005.09.033>, 2006.
- Zhi, W., Klingler, C., Liu, J., and Li, L.: Widespread deoxygenation in warming rivers, *Nat. Clim. Chang.*, 13, 1105–1113, <https://doi.org/10.1038/s41558-023-01793-3>, 2023.
- Zipper, S. C., Hammond, J. C., Shanafield, M., Zimmer, M., Datry, T., Jones, C. N., Kaiser, K. E., Godsey, S. E., Burrows, R. M., Blaszczyk, J. R., Busch, M. H., Price, A. N., Boersma, K. S., Ward, A. S., Costigan, K., Allen, G. H., Krabbenhoft, C. A., Dodds, W. K., Mims, M. C., Olden, J. D., Kampf, S. K., Burgin, A. J., and Allen, D. C.: Pervasive changes in stream intermittency across the United States, *Environ. Res. Lett.*, 16, 084033, <https://doi.org/10.1088/1748-9326/ac14ec>, 2021.